Stereoselective Aldol Additions Catalyzed by Dihydroxyacetone Phosphate-Dependent Aldolases in Emulsion Systems: Preparation and Structural Characterization of Linear and Cyclic Iminopolyols from Aminoaldehydes

Laia Espelt,[a, c] Teodor Parella,[e] Jordi Bujons,[b] Conxita Solans,[c] Jesús Joglar,[d] Antonio Delgado,[d, f] and Pere Clapés*[a]

Abstract: The potential of dihydroxyacetone phosphate (DHAP)-dependent aldolases to catalyze stereoselective aldol additions is, in many instances, limited by the solubility of the acceptor aldehyde in aqueous/co-solvent mixtures. Herein, we demonstrate the efficiency of emulsion systems as reaction media for the class I fructose-1,6-bisphosphate aldolase (RAMA) and class II recombinant rhamnulose-1-phosphate aldolase from *E. coli* (RhuA)-catalyzed aldol addition between DHAP and *N*-benzyloxycarbonyl (*N*-Cbz) aminoaldehydes. The use of emulsions improved the RAMA-catalyzed aldol conversions by three to tenfold relative to those in conventional DMF/water mixtures. RhuA was more reactive than RAMA towards the *N*-Cbz aminoaldehydes regardless of the reaction medium. With (*S*)- or (*R*)-Cbz-alaninal, RAMA exhibited preference for the *R* enantiomer, while RhuA had no enantiomeric discrimination. The linear *N*-Cbz aminopolyols thus obtained were submitted to catalytic intramolecular reductive amination to afford the corresponding iminocyclitols. This reaction was diastereoselective in all cases examined; the face selectivity was controlled by the stereochemistry of the newly formed hydroxyl group originating from the aldehyde. Characterization of the resulting iminocyclitols allowed the assessment of the diastereoselectivity of the enzymatic aldol reactions with respect to the *N*-protected aminoaldehyde. RAMA formed single diastereoisomers from *N*-Cbz-glycinal and from both enantiomers of *N*-Cbz-alaninal, while 14% of the epimeric product was observed from *N*-Cbz-3-aminopropanal. Diastereoselectivity from RhuA was lower than that observed from RAMA. Interestingly, a single diastereoisomer was formed from (*S*)-Cbz-alaninal, whereas only a 34% diastereomeric excess was observed from its enantiomer (i.e., (*R*)-Cbz-alaninal).

Keywords: biotransformations · colloids · DHAP-dependent aldolases · iminocyclitols · lyases

Introduction

The stereoselective carbon–carbon bond formation catalyzed by aldolases has attracted tremendous interest in recent years.[1, 2] In particular, dihydroxyacetone phosphate (DHAP)-dependent aldolases have been demonstrated to be extremely useful tools in the asymmetric synthesis of conventional and uncommon carbohydrates as well as other complex hydroxylated products. DHAP aldolases catalyze the aldol addition of the DHAP donor substrate to a variety of non-natural aldehyde acceptors and, in many cases, the stereoselectivity of the reaction is controlled by the enzyme, regardless of the structure and stereochemistry of the substrate acceptor.[3]

[a] Dr. P. Clapés, Dr. L. Espelt
Department of Peptide and Protein Chemistry
Institute for Chemical and Environmental Research-CSIC
Jordi Girona 18–26, 08034 Barcelona (Spain)
Fax: (+34)93-4006112
E-mail: pcsqbp@iiqab.csic.es

[b] Dr. J. Bujons
Department of Biological Organic Chemistry (DBOC)
Institute for Chemical and Environmental Research-CSIC
Jordi Girona 18–26, 08034 Barcelona (Spain)

[c] Dr. L. Espelt, Dr. C. Solans
Department of Surfactant Technology
Institute for Chemical and Environmental Research-CSIC
Jordi Girona 18–26, 08034 Barcelona (Spain)

[d] Dr. J. Joglar, Dr. A. Delgado
Research Unit on Bioorganic Molecules (RUBAM)
Department of Biological Organic Chemistry
Institute for Chemical and Environmental Research-CSIC
Jordi Girona 18–26, 08034 Barcelona (Spain)

[e] Dr. T. Parella
Servei de Ressonància magnètica Nuclear Universitat Autònoma de Barcelona, Bellaterra (Spain)

[f] Dr. A. Delgado
Unitat de Química Farmacèutica
Facultat de Farmacia, Universitat de Barcelona (Spain)

Supporting information for this article is available on the WWW under http://www.wiley-vch.de/home/chemeurj.org/ or from the author.

 DOI: 10.1002/chem.200304966

DHAP aldolases have been exploited as catalysts for the synthesis of glycoprocessing enzyme inhibitors such as polyhydroxy-*N*-heterocycles (iminocyclitols).[4–7] These compounds have been largely investigated as therapeutic targets for the design of new antibiotics, antimetastatic, antihyperglycemic, or immunostimulatory agents.[8–10] The key step of the chemoenzymatic synthesis of these products was the stereoselective carbon–carbon bond formation between DHAP and synthetic equivalents of aminoaldehydes. It has been shown that azido aldehydes or *N*-formamido aldehydes are the best substrates for fructose 1,6-diphosphate aldolase at synthetically practical rates.[4, 11] *N*-Formyl aminoaldehydes have the tremendous additional advantage that they can be obtained from the wide structural variety of readily available optically pure α- or β-amino acids and their derivatives.[12, 13] Nevertheless, the use of these substrates may be complicated by the racemization of the α stereogenic center observed with some derivatives,[14] which is probably mediated by the *N*-formyl group. Moreover, *N*-formyl deprotection conditions are not always compatible with sensitive compounds.[11]

Use of the well-known benzyloxycarbonyl (Cbz) or *tert*-butyloxycarbonyl (Boc) *N*-protecting groups for aminoaldehydes can be advantageous for two main reasons: 1) they constitute an excellent complement for orthogonal protection schemes in particular when the aldol adducts obtained are to be used as chiral building blocks, and 2) the urethane-type protecting groups may be less prone to spontaneous racemization of the stereogenic center(s). *N*-Cbz aminoaldehydes were found to be poor substrates for fructose 1,6-diphosphate aldolase.[4, 11, 15–17] Only the products formed from *N*-(Cbz)aminoacetaldehyde (i.e., Cbz-glycinal), *N*-(Cbz)-3-aminopropanal, and DHAP have been characterized although these were obtained in low yields.[15, 17] Some authors suggested that either the size of the *N*-substituent or their poor water solubility might account for the low reactivity observed.[4, 11, 16–18] Moreover, increasing the percentage of organic co-solvent in the medium to make the aldehyde soluble may lead to either a dramatic enzyme deactivation[19] or an insolubilization of the DHAP sodium salt. As a result, no reaction or insufficient product yields are often obtained.

In the present study we endeavored to gain insight into the reactivity of *N*-(Cbz)-protected aminoaldehydes as substrates for the aldolase-catalyzed stereoselective synthesis of polyhydroxylated amines. To this end, we have recently developed new reaction systems based on colloidal dispersions,[20, 21] namely highly concentrated water-in-oil (gel) emulsions, which overcome most of the disadvantages of the aqueous/co-solvent mixtures such as inactivation of the aldolase and incomplete aldehyde solubilization in the medium. These reaction systems consist of ternary mixtures of water (e.g., 90% w/w), a dispersant agent of the poly(oxyethyleneglycol alkyl ether)-type (e.g., 4% w/w), and an aliphatic hydrocarbon (e.g., 6% w/w).[22]

The goal of the present work was to explore whether the solubility or structural properties of the *N*-(Cbz)-protected aminoaldehydes were responsible for their poor reactivity as acceptor substrates in aldolase-catalyzed condensations. For this purpose, the reactions were carried out in the aforementioned high water content emulsions to ensure both a good solubilization of the aldehyde and an effective contact with the enzyme. For the sake of comparison, a reaction medium based on co-solvent mixtures such as dimethylformamide (DMF)/water 1:4 was also assayed. Furthermore, another goal was to elucidate the stereochemistry of both the linear adducts and the corresponding cyclic products (iminocyclitols) to assess the stereoselectivity of the aldolases used towards the newly formed carbon–carbon bond. We selected the following acceptor aldehydes: benzyl 3-oxopropylcarbamate (**5**), benzyl 3-oxoethylcarbamate (Cbz-glycinal) (**6**), (*S*)-benzyl 1-methyl-2-oxoethylcarbamate ((*S*)-Cbz-alaninal) (**7**), and (*R*)-benzyl 1-methyl-2-oxoethylcarbamate ((*R*)-Cbz-alaninal) (**8**). Type I D-fructose-1,6-diphosphate aldolase from rabbit muscle (RAMA) and type II recombinant L-rhamnulose-1-phosphate aldolase (RhuA) from *E. coli* were the biocatalysts.

Results and Discussion

In previous work on aldolase-catalyzed reactions in water/organic solvent (W/O) gel emulsions, we concluded that the partition coefficient of the acceptor aldehyde between both the continuous (i.e., water) and dispersed phase (i.e., aliphatic hydrocarbon also referred to as the oil) as well as the water–oil interfacial tension were the parameters that control both the enzymatic activity and product yield.[21] These parameters were strongly affected by the nature of the aliphatic hydrocarbon and the acceptor aldehydes, while no influence was observed by either the DHAP or the enzyme. Thus, the best reaction systems were W/O gel emulsions formulated with water (90 wt%), technical-grade tetraethylene glycol tetradecyl ether surfactant ($C_{14}H_{29}(OCH_2CH_2)_4OH$) (4 wt%), with an average of 4 moles of ethylene oxide per surfactant molecule, abbreviated as $C_{14}E_4$, and an aliphatic hydrocarbon (6 wt%) such as tetradecane (C_{14}) or hexadecane (C_{16}). Interestingly, the stability of the fructose-1,6-diphosphate aldolase from rabbit muscle (RAMA) in the presence of 50 mM phenylacetaldehyde, a low water-soluble aldehyde, was 25-fold higher in gel emulsions than in a DMF/water 1:4 (v/v) mixture. In this work, we used these emulsion systems to perform the enzymatic aldol additions between DHAP and *N*-Cbz aminoaldehydes.

Preparation of *N*-protected aminoaldehydes: The *N*-Cbz aminoaldehydes were synthesized from the corresponding amino alcohols. These were first protected as Cbz derivatives followed by oxidation of the alcohol function (Scheme 1). For the protected amino alcohols **1** and **2**, the Swern oxidation was the method of choice, whereas for both enantiopure **3**[23] and **4** the methodology using 2-iodoxybenzoic acid (IBX)[24] was preferred.[25] Both methods gave 90–95% oxidation yields. In most instances, a simple workup followed by a rough crystallization or precipitation provided the aminoaldehydes in a form pure enough to be used in the enzymatic aldol condensation. An exception was the *N*-protected aminoaldehyde **6**. In this case, the product did not crystallize and purification by reversed-phase HPLC was required.

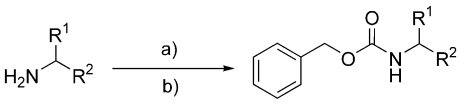

1 R^1: H, R^2: CH_2CH_2OH
2 R^1: H, R^2: CH_2OH
3 R^1: (*S*) CH_3, R^2: CH_2OH
4 R^1: (*R*) CH_3, R^2: CH_2OH
5 R^1: H, R^2: CH_2CHO
6 R^1: H, R^2: CHO
7 R^1: (*S*) CH_3, R^2: CHO
8 R^1: (*R*) CH_3, R^2: CHO

Scheme 1. Synthesis of acceptor aldehydes **5**–**8**: a) Cbz-OSu dioxane/H_2O 4/1; b) Swern or IBX oxidation.

Enzymatic aldol reactions: First, we chose the RAMA-catalyzed aldol condensation of DHAP with the acceptor aminoaldehyde **5** to test the emulsion media (see Table 1). It is worth stressing that the reaction performance in gel emulsions at 25 °C with $C_{14}E_4$ as surfactant may depend on both the physicochemical characteristics of the acceptor aldehyde (e.g., hydrophobicity and solubility) and the aliphatic hydrocarbon used to formulate the emulsion.[21] Thus, as mentioned before, the reactions were conducted in the best emulsions of the ternary water/$C_{14}E_4$/oil (90/4/6 wt %) systems, in which the oil component was tetradecane, hexadecane, or squalane (C_{30}).[26] The reaction conversion to **9** was also examined as a function of DHAP concentration (30 mM and 120 mM) with 1.7 equiv mol^{-1} of *N*-aminoaldehyde. For the sake of comparison, the reactions were also conducted in a conventional DMF/water 1:4 (v/v) co-solvent mixture.[27]

The maximum reaction conversions to **9** obtained in emulsion media and the DMF/water 1:4 mixture are summarized in Table 1. At 30 mM DHAP and 1.7 equiv mol^{-1} of acceptor aldehyde, the best yields were achieved in emulsions formulated with either tetradecane or hexadecane and in the DMF/water 1:4 (v/v) mixture. This indicates that *N*-Cbz-aminoaldehyde **5** was accepted by RAMA at rates good enough for preparative-scale reactions. Interestingly, at 120 mM DHAP the reaction conversion to **9** achieved in emulsion media was threefold higher than that in the DMF/water 1:4 mixture (Table 1, entries 1, 3, and 6). In the latter medium, the reaction turned out to be impractical for preparative purposes. These differences in the reaction efficiency appeared to be related to both the limited solubility of the acceptor aldehyde[4, 17] and the stability of the enzyme. The solubility of **5** in the DMF/water 1:4 mixture was measured experimentally and was around 144 mM. Therefore, the effective molar ratio of aldehyde/DHAP (144:120) was only 1:1.2. Hence, the lower substrate molar ratio caused by the limited solubility of acceptor aldehyde is one factor that might explain the poor conversions achieved in the DMF/water 1:4 mixture. To demonstrate this, we examined the influence of the number of molar equivalents (equiv mol^{-1}) of aldehyde acceptor used on the reaction conversion to **9**. To this end, experiments were conducted in emulsion media to ensure good solubilization of the aldehyde. On increasing the aldehyde concentration up to 3 equiv mol^{-1} the conversion improved slightly (see Table 1, entries 2 and 4). In contrast, at equimolar aldehyde/DHAP ratio the conversion dropped to approximately 40 %.

A second factor that may reduce the effectiveness of the DMF/water mixtures was the enzyme stability. Thus, the enzyme activity may be extinguished before the reaction reached equilibrium. However, in this case, by increasing the enzyme concentration up to threefold (i.e., from 12 to 35 U mL^{-1}) the conversion increased from 21 % (Table 1, entry 6) to only a modest 38 %, which was also the maximum found for an equimolar aldehyde/DHAP ratio (see above).

An important feature to consider was the evolution of the aldol condensation product with the reaction time. Analysis of the reaction progress indicated a fast conversion to **9** reaching a maximum followed by a gradual decreased for prolonged incubation times (Figure 1) (10 % conversion to **9** after 120 h of incubation). It is worth stressing that DHAP is not stable, especially at elevated pH values, and decomposes into methylglyoxal.[28, 29] Moreover, the aldehyde is also in equilibrium with its hydrate form and with other polymeric forms which can vary with the reaction progress.[30] Although a satisfactory explanation has not yet been found, the observed consumption of **9** was presumably due to the spontaneous decomposition of the DHAP, the aldehyde, or both. Consequently, the reaction equilibrium shifted to the reactants in a retro-aldol-type reaction. As depicted in Figure 1, this effect was much more evident in emulsion media than in the DMF/water 1:4 mixture. This was attributed to the enzyme activity, since the enzyme half-life was 25-fold higher in emulsions

Table 1. RAMA-catalyzed aldol addition between DHAP and **5**.

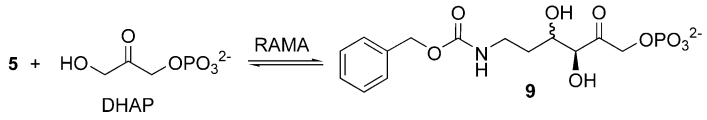

Entry	Reaction medium[b]	Aldehyde [equiv mol^{-1}]	Conversion [%][a] (Time [h]) 30 mM DHAP[c]	120 mM DHAP[d]
1	water/$C_{14}E_4$/tetradecane	1.7	60(4.5)	60(1)
2	water/$C_{14}E_4$/tetradecane	3	–[e]	65(1)
3	water/$C_{14}E_4$/hexadecane	1.7	64(4.5)	60(1)
4	water/$C_{14}E_4$/hexadecane	3	–[e]	62(1)
5	water/$C_{14}E_4$/squalane	1.7	51(1)	53(1)
6	DMF/water 1:4 v/v	1.7	64(4.5)	21(24)

[a] Molar percentage conversion to **9** (with respect to the starting DHAP concentration) determined by HPLC from the crude reaction mixture using purified standard. [b] Reaction volume 2.5 mL, $T = 25$ °C, 90/4/6 wt %, respectively, in emulsion. [c] [RAMA] = 5 U mL^{-1}. [d] [RAMA] = 12 U mL^{-1}. [e] Not determined.

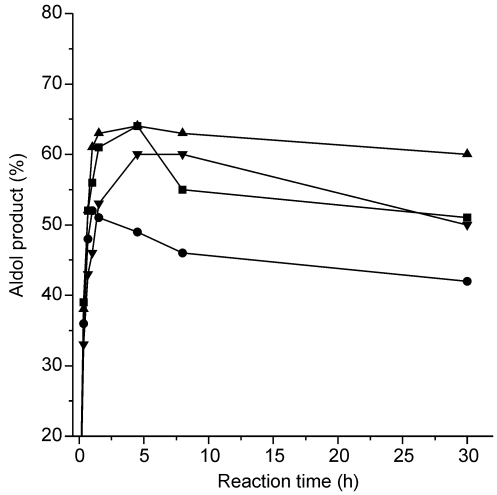

Figure 1. RAMA-catalyzed aldol reaction between DHAP and **5**. Reaction time-course of product **9** formation in water/$C_{14}E_4$/oil 90:4:6 wt% emulsion systems in which the oil component was tetradecane (▼), hexadecane (■), squalane (●), and DMF/water 1:4 v/v mixtures (▲). [DHAP] = 30 mM, 1.7 equiv mol^{-1} of **5**, reaction volume 2.5 mL, and [RAMA] = 5 U mL^{-1}. Reactions were carried out as described in the Experimental Section

than in the DMF/water 1:4 mixture (100 h versus 4 h),[21] which therefore allowed secondary reactions to occur.

The extension of this phenomenon was difficult to generalize, since it may also depend on the reaction product. Hence, both the reaction time and the amount of enzyme must be controlled to achieve the maximum yields and avoid the retro-aldol reaction. In this work, each reaction was monitored by HPLC and the maximum conversions of product are given.

Synthetic applications

Influence of the acceptor aldehyde and the reaction medium: The next step was to test the versatility of the novel reaction medium with some more examples. We chose Cbz-glycinal (**6**), (*S*)-Cbz-alaninal (**7**), and (*R*)-Cbz-alaninal (**8**) as acceptor aldehydes in addition to benzyl 3-oxopropylcarbamate (**5**) using RAMA and recombinant L-rhamnulose-1-phosphate aldolase (RhuA) from *E. coli* as catalysts. Reactions were performed in emulsions and in the DMF/water 1:4 (v/v) mixture. For the sake of simplicity, we will first discuss the reactivity of the aldolases as a function of both the *N*-aminoaldehyde and the reaction medium; the structural and stereochemical characterization of the products obtained will be analyzed in detail later.

Reaction conversions obtained are summarized in Table 2. It is clear that the *N*-Cbz aminoaldehydes tested were accepted as substrates for RAMA and RhuA aldolases. Overall, RhuA was more active than RAMA; the reactions catalyzed by the latter were influenced much more by the type of reaction media (Table 2, entries 1–3). This result could be explained partially by the observed higher affinity of RhuA

Table 2. RAMA- and RhuA-catalyzed aldol addition between DHAP and *N*-Cbz-aminoaldehydes.

Entry	Acceptor aldehyde	Aldolase [U mL^{-1}]	Conversion [%][a] (Time [h]) Reaction conditions[b] A[c]	B[d]	C[e]	D[f]	Product[g]
1	**6**	RAMA (10)	76(24)	82(24)	83(24)	27(24)	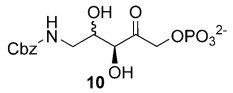 **10**
2	**7**	RAMA (23)	20(46)	18(46)	18(46)	4(46)	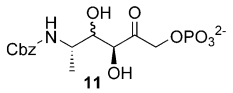 **11**
3	**8**	RAMA (21)	40(24)	40(24)	56(24)	5(24)	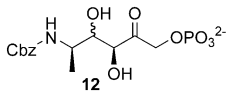 **12**
4	**5**	RhuA (1)	50(4)	48(2)	47(4)	58(7)	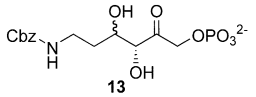 **13**
5	**6**	RhuA (1)	84(1)	96(1)	80(3)	80(3)	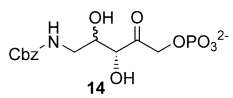 **14**
6	**7**	RhuA (1)	66(2)	59(2)	66(5)	60(2)	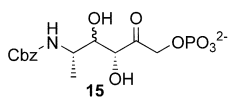 **15**
7	**8**	RhuA (1.3)	67(2)	74(4)	67(4)	61(4)	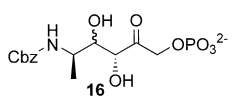 **16**

[a] Molar percentage conversion to the aldol adduct (**10**–**16**) (with respect to the starting DHAP concentration) determined by HPLC from the crude reaction mixture using purified standards. [b] The initial concentration of the DHAP was in the range 90–120 mM, reaction volume 5 mL, $T = 25\,^{\circ}C$. [c] H_2O/$C_{14}EO_4$/tetradecane 90/4/6 wt%. [d] H_2O/$C_{14}EO_4$/hexadecane 90/4/6 wt%. [e] H_2O/$C_{14}EO_4$/squalane 90/4/6 wt%. [f] DMF/H_2O 1:4 v/v. [g] For C-4 stereochemistry, see text.

for both nonpolar and sterically hindered substrates relative to that of RAMA.[28, 31]

Besides the substrate preferences, the emulsion media enhanced the catalytic efficiency of RAMA towards hydrophobic substrates such as the *N*-Cbz aminoaldehydes tested by three-, five-, and even tenfold, thereby allowing the synthesis of the corresponding products at preparative level in moderate to good yields. In contrast, in the DMF/H_2O 1:4 (v/v) mixture, the *N*-Cbz aminoaldehydes were poor substrates for RAMA. It is worth mentioning that in DMF/H_2O 1:4 (v/v), the conversion to **10** improved up to 60% upon increasing the RAMA concentration by 3.5-fold (i.e., up to 35 U mL^{-1}). On the other hand, with aldehydes **7** and **8** no improvement in the conversion was observed when raising the concentration of aldolase. These results reinforce the fact that both the solubility of the aldehyde and the stability of the aldolase may play a major role in the efficacy of the DMF/H_2O system (see previous section).

These results indicate that the reaction performance may be affected not only by structure of the aminoaldehyde but also by the reaction medium. However, this was also a function of the aldolase used. Thus, reactions with RhuA, a type II aldolase, gave good results regardless of the reaction media (Table 2, entries 4–7). This behavior may be related to both its higher tolerance towards hydrophobic substrates and its high stability in the presence of organic polar solvents.[31] It is noteworthy that the reaction profiles with aldehydes **5** and **6** showed, for both enzymes, the phenomenon of the retro-aldol reaction described above. Hence, conversion to the product decreased by 10–30% after 24 h depending on both the reaction conditions and the aldehyde. Interestingly, this phenomenon was not observed for the reactions with the acceptor aldehydes **7** and **8**.

We found that RAMA exhibited a moderate preference towards the (*R*)-Cbz-alaninal (**8**) over the (*S*)-Cbz-alaninal (**7**) (Table 2, entries 2 and 3). The reverse situation was reported by Hung et al.,[11] who found that RAMA preferred the *S* enantiomer of a series of *N*-α-amino protected-β-hydroxypropanals as aldehyde acceptors. On the other hand, RhuA showed no preference for any of the enantiomers of Cbz-alaninal (Table 2, entries 6 and 7). In contrast, high kinetic enantiodiscrimination by this aldolase has been reported with a series of racemic 2-hydroxyaldehydes acceptors.[32]

To explain the observed preference of RAMA towards the *R* isomer of Cbz-alaninal, a computational model was constructed. Although a detailed study of this kind is beyond the scope of this work, the preliminary model presented may help to elucidate the different binding modes to the protein of both isomers of Cbz-alaninal and those of their reaction products with DHAP. Based on the known mechanisms of class I and II DHAP-dependent aldolases[33, 34], we looked at the states before and after the carbon–carbon bond formation (I and II in Scheme 2).

Figure 2A shows the compared minimized structures obtained for the *R* and *S* enantiomers of Cbz-alaninal in state I. These structures were generated by imposing a restraint during the minimization process to keep the distance between C-3 of the bound DHAP and C-1 of Cbz-alaninal close to 2.5 Å. The purpose of this arbitrarily chosen restraint was to ensure that the aldehyde molecule would adopt a conformation close to the pre-reaction state. In this situation, both enantiomers of the aldehyde show very similar conformations stabilized by hydrogen bonds with several amino acids that are in the catalytic site. In particular, the one between the aldehyde oxygen atom and the protonated carboxylic group of Asp33 fixes the orientation of the aldehyde group to approach from its *si* face to the reactive enamine derived from the DHAP moiety. This model does not exclude the possibility that other residues located by the C-terminus of RAMA (i.e., Tyr363) could participate in the enzymatic mechanism by orienting and promoting proton transfer to the aldehyde, as has been suggested in the literature.[35, 36] The enamine C-3 hydroxyl group is also kept in its reactive orientation by hydrogen bonds to Glu187 and Asp33. Although there are no obvious interactions between the methyl group at C-2 of the isomers of Cbz-alaninal and the protein, there is a difference in the energy calculated for both

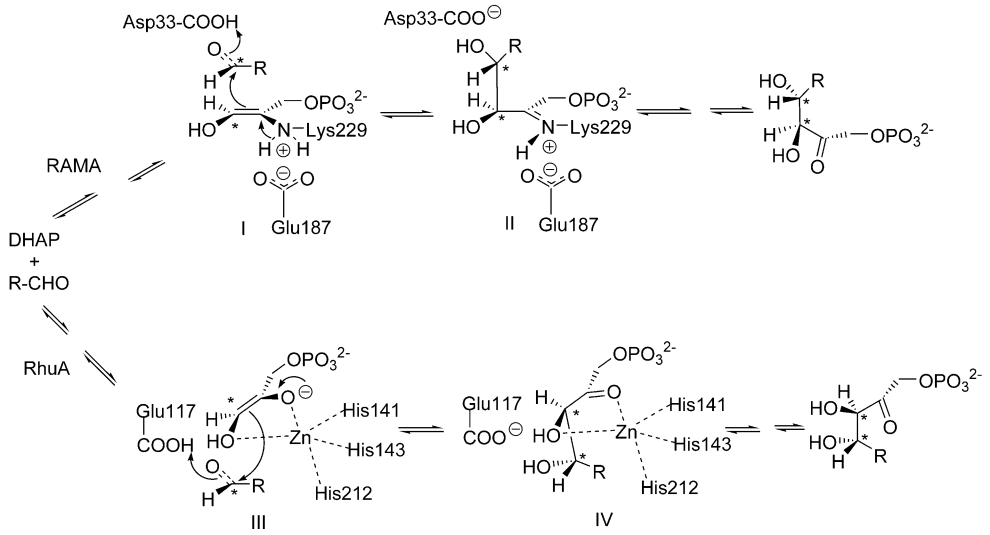

Scheme 2. Formation of the C–C bond in the reactions catalyzed by a class I aldolase (RAMA) and a class II aldolase (RhuA).

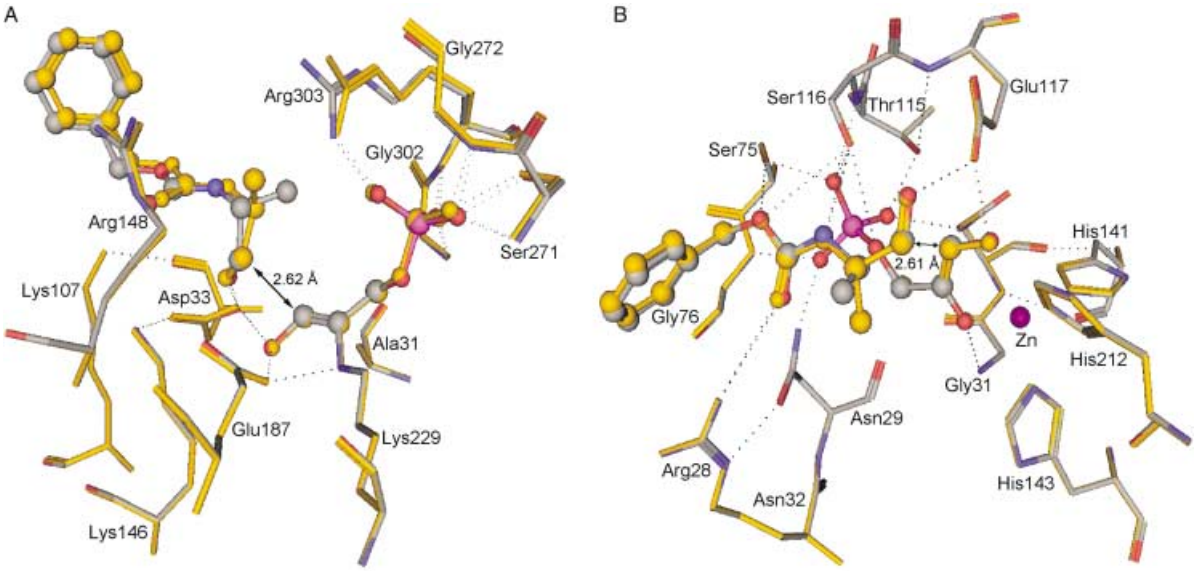

Figure 2. Structure of the active site of RAMA (A) and RhuA (B) complexed to DHAP and both isomers of Cbz-alaninal (state I and III, respectively). The conformations of the active site residues (sticks) and of the substrates (ball-and-stick) are represented in different colors: the complexes with *R*-Cbz-alaninal are represented using gray for the carbon atoms, blue for the nitrogen atoms, red for the oxygen atoms, while the complexes with the *S* isomer are represented with all atoms in orange. The distance between the two carbon atoms that participate in bond formation is shown for each case.

isomers complexed to the protein; these are lower for the *R* isomer ($\Delta E^{R-S} = -2.2$ kcal mol^{-1}). This difference is kept even if the restraint imposed during the minimization is removed and the aldehyde is allowed to relax to a new energetic minimum about 3.5 Å away from the DHAP moiety. These energy differences arise from a sum of small contributions from different interactions between the substrates and the protein bound to DHAP. Similarly, the structures (not shown) obtained for each adduct in state II (Scheme 2) show a small difference in energy that favors the one derived from *R*-Cbz-alaninal ($\Delta E^{R-S} = -1.6$ kcal mol^{-1}).

These differences suggest that the *R* isomer of Cbz-alaninal forms a more stable complex with the DHAP-modified protein than the *S* isomer. Similarly, the adduct formed with *R* configuration at C-5 seems to be more stable than the one with the *S* configuration. However, these differences do not necessarily explain our experimental observations, since we have only looked at one of the steps of the multistep enzymatic mechanism that is proposed for this aldolase.

The same type of study for the complexes of *R*- and *S*-Cbz-alaninal with DHAP-ligated RhuA (state III, Scheme 2) gave the results shown in Figure 2B. Similarly, the orientation of the aldehyde group is fixed by a hydrogen bond interaction with the protonated carboxylic group of Glu117, which also interacts with the hydroxyl group on C-3 of the DHAP molecule complexed to the Zn^{2+} ion. This interaction forces the approach of the aldehyde to the DHAP-enolate from its *re* face. Energetically, the *R* isomer of Cbz-alaninal is again favored over the *S* isomer ($\Delta E^{R-S} = -9.0$ kcal mol^{-1}) and the same applies for the complex once the carbon–carbon bond between the aldehyde and DHAP is formed ($\Delta E^{R-S} = -8.6$ kcal mol^{-1}). Again, these differences cannot be attributed to a specific interaction of any of the groups present in the organic ligands with the protein.

Purification and structural and stereochemical characterization of the aldol adducts: Compounds **9**–**16** were synthesized on the milligram scale (50–160 mg) and purified by a combination of ion exchange and reverse-phase (RP) HPLC methodologies. The RP-HPLC was mostly a desalting step and, as observed by analytical RP-HPLC, separation of the putative diastereoisomers was not accomplished under these conditions. This two-step purification procedure provided product recoveries, without any optimisation, ranging from 55 to 75 %. The purity was assessed by both HPLC and elemental analysis.

The structural and stereochemical characterization of the products was ascertained by one- and two-dimensional NMR techniques. Assignments of relative configurations of acyclic structures by NMR-based methods are elusive in most instances, since their rotational freedom leads to multiple conformers.[37] We therefore studied the stereochemical structure of both linear and the corresponding cyclic compounds, namely iminocyclitols or iminosugars. The latter are important biologically active compounds and are among the most effective glycosidase inhibitors.

To obtain more simple NMR spectra, in some instances the phosphate group of compounds **9**–**16** was removed by treatment with acid phosphatase followed by desalting by RP-HPLC. The structural features of these compounds were found to be independent of the presence of the phosphate moiety. The NMR data from **9** and **13** revealed that one major conformer with H_3/H_4-*syn* orientation was present (i.e., small values of ^3J(H-3,H-4), ^3J(C-2,H-4), ^3J(C-5,H-3) and NOE (H-4,H-3) strong) (Scheme 3).

Hence, the relative stereochemistry at C-3 and C-4 carbons is consistent with that proposed for RAMA and RhuA catalysis, respectively.[1, 31, 38] Based on mechanistic considerations of the DHAP aldolases[31, 34, 39–41] it can be assumed that the absolute configuration at C-3 is independent on the

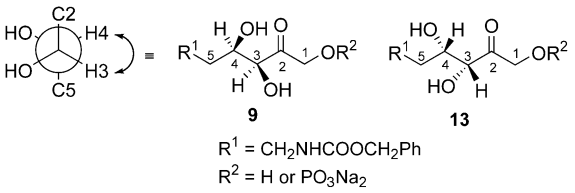

Scheme 3. Main conformer of compounds **9** and **13**.

acceptor used in the reaction. Moreover, optical rotations of **9** and **13** have opposite signs (Table 3, entries 1 and 5). Thus, the absolute configurations 3*S*,4*R* and 3*R*,4*S* can be assigned for **9** and **13**, respectively. In addition to the expected products **9** and **13**, minor signals (8%) corresponding to a cyclic hemiaminal, as confirmed from the NOESY and HMBC spectra, were detected.[42] This compound resulted from the reversible spontaneous intramolecular addition of the secondary amino group to the ketone carbonyl without formation of the corresponding enamine (Scheme 4).

For compounds **10**–**12** and **14**–**16** even more complex NMR spectra were obtained, which made it extremely difficult to unequivocally assign the relative configuration at C-3 and C-4 as well as to identify and quantify the putative diastereoisomers. By analogy with compounds **9** and **13**,

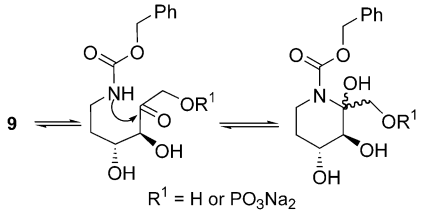

Scheme 4. Spontaneous intramolecular cyclization of **9**.

Table 3. Structure of the cyclic iminocyclitols derived from linear compounds **9**–**16**.

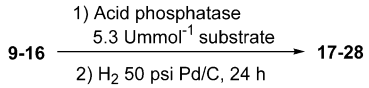

Entry	Acceptor aldehyde/ aldolase	Linear product/ $[\alpha]_D^{20}$ ($c=1$ in MeOH)	Cyclic products	C-3, C-4 Stereochemistry [*trans*/*cis* ratio]	$[\alpha]_D^{20}$ Cyclic product or mixture
1	**5** RAMA	**9**/+16.2	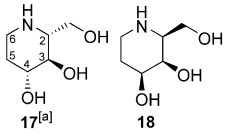 **17**[a] **18**	86/14	+8.2 ($c=1.4$ in MeOH)
2	**6** RAMA	**10**/+1.1	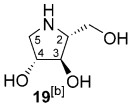 **19**[b]	*trans* only	+18.7 ($c=1$ in MeOH)
3	**7** RAMA	**11**/−9.2	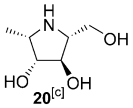 **20**[c]	*trans* only	+16.0 ($c=0.4$ in MeOH)
4	**8** RAMA	**12**/−1.8	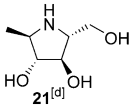 **21**[d]	*trans* only	+45.0 ($c=1.4$ in MeOH)
5	**5** RhuA	**13**/−11.6	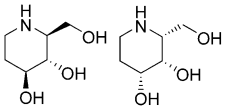 **22** **23**	80/20	−6.0 ($c=1.5$ in MeOH)
6	**6** RhuA	**14**/−0.2	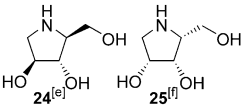 **24**[e] **25**[f]	90/10	−18.0 ($c=1.5$ in MeOH)
7	**7** RhuA	**15**/−1.4	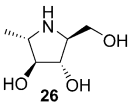 **26**	*trans* only	−33.0 ($c=1.2$ in MeOH)
8	**8** RhuA	**16**/+7.8	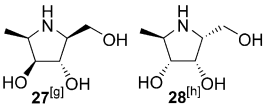 **27**[g] **28**[h]	67/33	−11.0 ($c=1$ in MeOH)

[a] References [58–62]. [b] References [60, 61, 63–66]. [c] References [67, 68]. [d] References [47, 67, 69–71]. [e] References [60, 61, 72–78]. [f] References [58, 77, 79–81]. [g] References [47, 70]. [h] References [82].

variable-temperature NMR experiments and exchange peaks observed in NOESY experiments of **10** (or its enantiomer **14**) revealed that both linear and cyclic structures were in equilibrium, but in this case at equimolar concentrations (Scheme 5). The major conformer of the linear product (**10a**) was similar to the one found for compound **9** and it was

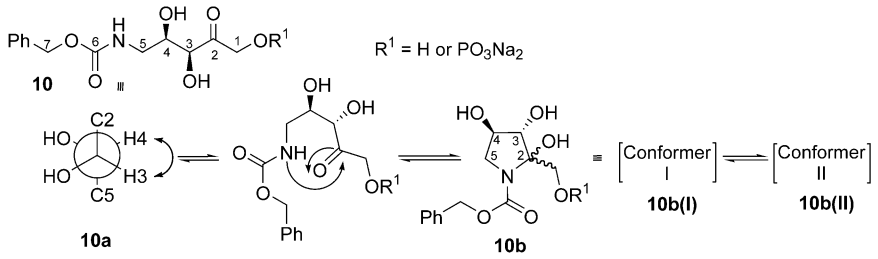

Scheme 5. Main conformer and spontaneous intramolecular cyclization of **10** with or without the phosphate group.

consistent with the stereochemistry of RAMA catalysis. Moreover, the cyclic compound **10b** also showed another additional equilibrium between two other equally populated conformations (**10b(I)** and **10b(II)**), presumably due to the pseudorotation commonly observed in five-membered nitrogen-containing rings (Scheme 5).[43] The spontaneous formation of the cyclic compounds and their conformational equilibrium was also confirmed by observing the ^{1}H NMR and two-dimensional NOESY spectra at different temperatures.[44]

The presence of linear and cyclic species in equilibrium may explain the low and unexpected values of the optical rotations found for some enantiomeric products (Table 3, entries 2–4, and 6–8). The spontaneous cyclization would also explain the chromatographic behavior of these products on reversed-phase HPLC analysis: either broad peaks or two peaks without baseline recovery between them were observed, suggesting a slow equilibrium between two or more species.

As indicated above, the cyclic compounds, namely iminocyclitols, were also obtained and structurally characterized. To this end, the phosphate group of compounds **9**–**16** was removed and the resulting products were hydrogenated following the procedure described in the Experimental Section.[45] During this step, we assumed, according to the literature data,[6, 17, 46] that the stereochemistry at C-3 and C-4 was conserved and that no epimerization occurred. Aqueous solutions of the iminocyclitol in its free-base form were adjusted to pH 6.5, lyophilized, and submitted to NMR analysis without any further purification process.

This allowed us to identify unequivocally and quantify the diastereoisomers thus formed and therefore to elucidate the stereoselectivity of the enzymatic aldol condensation towards the aldehyde acceptor. The identified cyclic products from the corresponding linear compounds are depicted in Table 3. Most of them are well described in the literature (Table 3) and have been either isolated from natural sources or synthesized by chemical or chemoenzymatic methodologies. Remarkably, to the best of our knowledge, iminocyclitols **22** and **26** and the minor products **18** and **23** have been obtained and characterized for the first time in this work. Compound **27** had been isolated from the bark of *Angylocalyx pynaertii* (*Leguminosae*)[47] and its synthesis is presented here for the first time.

In addition to NOE data, the shielding effects observed on some proton and carbon chemical shift values due to the spatial effect of the adjacent hydroxyl groups have been used as a probe to determine and assign the relative stereochemistry in these families of compounds, especially for the five-membered rings (Tables 4 and 5). As a general trend, a deshielding effect was observed on the chemical shift of both proton and carbon depending on the stereochemistry of the contiguous hydroxyl substituents. The hydroxyl groups OH(3) and OH(4) in compounds **19** and **24** induced 0.2–0.3 ppm upfield shift on the H-2, H-3, and H-4 protons compared with those of **25** due to their relative proximity, and therefore, *cis* stereochemistry. On the other hand, the reverse effect is observed on the C-2, C-3, and C-4 carbon centers, for which a 3–6 ppm upfield effect was observed. The anisotropic effect on the methyl carbon resonance is also important in compounds **28** and **27** (or its enantiomer **20**). In the case that OH(4) and Me(6) show a *cis* stereochemistry, a strong upfield effect of about 4–5 ppm was observed. All these predictions were further confirmed by NOE data.

An inspection of the stereochemistry at C-2 for the iminocyclitols described in Table 3 revealed that the reductive amination with Pd/C was highly diastereoselective, as reported previously by other authors.[4, 6, 15, 17, 38, 46] Interestingly, we have found that in both six- and five-membered ring systems, hydrogenation took place from the face opposite to the C-4

Table 4. ^{1}H and ^{13}C chemical shifts [ppm] of the five-membered iminosugars **19**, **24**, and **25**.

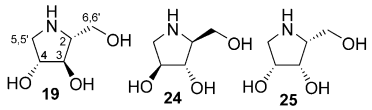

Product	δ(H/C)2	δ(H/C)3	δ(H/C)4	δ(H/C)5	δ(H/C)5′	δ(H/C)6	δ(H/C)6′
19/24	3.3/66.6	3.9/76.5	4.2/75.1	3.4/50.2	3.1/50.2	3.8/59.7	3.7/59.7
25	3.6/63.2	4.2/70.5	4.4/70.7	3.4/47.9	3.1/47.9	3.9/58.4	3.8/58.4

Table 5. ^{1}H and ^{13}C chemical shifts [ppm] of the five-membered iminosugars **20**, **21**, and **26**–**28**.

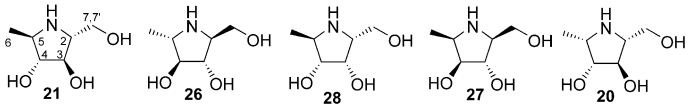

Product	δ(H/C)2	δ(H/C)3	δ(H/C)4	δ(H/C)5	δ(H/C)6	δ(H/C)7	δ(H/C)7′
21/26	3.3/62.4	3.3/75.8	3.7/80.3	3.3/57.3	1.3/15.4	3.8/59.6	3.7/59.6
28	3.7/61.5	4.3/70.4	3.9/76.7	3.5/56.7	1.3/15.0	3.9/58.4	3.8/58.4
27/20	3.5/67.5	4.0/76.3	4.1/76.3	3.7/58.3	1.3/10.7	3.8/59.6	3.7/59.6

hydroxyl group, regardless of the relative stereochemistry of the other substituents (Scheme 6). Hence, the stereochemistry observed at C-2 was controlled exclusively by the configuration at C-4.

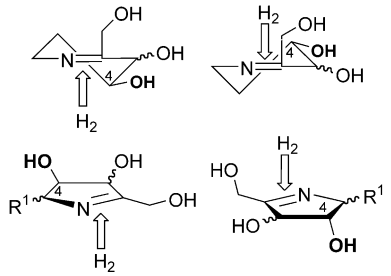

Scheme 6. Diastereoselectivity of the reductive amination for **9**–**16**.

Analysis of the stereochemistry at C-4 of iminocyclitols **17**–**27** (Table 3) can be used to infer, within the limits of detection by high-field ^{1}H NMR, the stereoselectivity of the aldolases towards each of the *N*-protected aminoaldehydes. As can be seen in Table 3 (entries 2–4), RAMA exhibited high stereoselectivity forming single cyclic diastereoisomers from aldehydes **6**–**8**. Condensation with aldehyde **5** afforded 14% of a minor diastereoisomer (Table 3, entry 1), arising from the *re*-face attack of the DHAP–RAMA complex on the aldehyde. This finding has also been observed with a series pyridine carbaldehydes and diethylaminoacetaldehyde.[28]

Class II RhuA was less diastereoselective than RAMA for the substrates assayed. Formation of diastereoisomers, epimeric at C-4, has also been reported with a series of nonpolar aliphatic aldehydes.[31] In the present study, the diastereoselectivity observed depended on both the structure and the stereochemistry of the *N*-Cbz aminoaldehyde. Aldehydes **5**, **6**, and **8** gave 10–33% of adducts arising from the reverse *si*-face attack on the aldehyde during the enzymatic aldol condensation (Table 3, entries 5, 6, and 8). Interestingly, the reaction with (*S*)-Cbz-alaninal (**7**) gave exclusively the expected stereochemistry (Table 3, entry 7), whereas its enantiomer **8** gave the lowest diastereoisomeric ratio (34% *de*)(Table 3, entry 8).

The major iminocyclitols obtained from RAMA- and RhuA-catalyzed reactions are enantiomers, in agreement with the optical rotations of the pure compounds and the diastereoisomeric mixtures (Table 3). It is also worth mentioning that the reaction media did not influence the stereoselectivity of the reactions.

Conclusion

In summary, the physicochemical characteristics of the reaction medium are of paramount importance for the enzymatic activity and reaction yield in aldolase-catalyzed stereoselective carbon–carbon bond formation. In this sense, emulsion-based reaction systems are a promising approach to overcome the problems facing the conventional aqueous/cosolvent mixtures when using water-insoluble substrates. In the particular case of *N*-Cbz aminoaldehydes, we have demonstrated that, in most instances, the low yields obtained are not exclusively due to the structural features of the acceptor aldehyde, but to its solubility as well. With the use of emulsion-based reaction systems it is possible to increase the efficiency of the aldolase-catalyzed carbon–carbon bond formation with insoluble substrates. Besides the reaction media, RhuA had higher reactivity towards the *N*-Cbz aminoaldehydes than RAMA, whereas the stereoselectivity of the aldol reaction was higher for the latter. With the *N*-Cbz aminoaldehydes tested, the stereoselectivity of RhuA depended on both the structure and stereochemistry of the acceptor aldehyde.

Experimental Section

Materials: Fructose-1,6-diphosphate aldolase from rabbit muscle (RAMA; EC 4.1.2.13, crystallized, lyophilized powder, 19.5 U mg^{-1}) was from Fluka (Buchs, Switzerland). Rhamnulose-1-phosphate aldolase (RhuA; EC 4.1.2.19, 100 U mL^{-1}) was kindly donated by Boehringer Mannhein (Mannheim, Germany). Acid phosphatase (PA, EC 3.1.3.2, 5.3 U mg^{-1}) was from Sigma (St. Louis, USA). Nonionic polyoxyethylene ether surfactant with an average of 4 moles of ethylene oxide per surfactant molecule ($C_{14}E_4$) was from Albright and Wilson (Barcelona, Spain). MacroPrep High Q Support anion-exchange resin was from BioRad (Hercules, USA). The precursor of dihydroxyacetone phosphate (DHAP), dihydroxyacetone phosphate dimer bis(ethyl ketal), was synthesized in our lab by a procedure described by Jung et al.[48] with slight modifications. Deionized water was used for preparative HPLC and Milli-Q-grade water for both analytical HPLC and gel emulsion formation. All other solvents and chemicals used in this work were of analytical grade.

HPLC analyses: HPLC analyses were performed on an RP-HPLC cartridge, 250 × 4 mm filled with Lichrosphere® 100, RP-18, 5 μm from Merck (Darmstadt, Germany). Samples (50 mg) were withdrawn from the reaction medium, dissolved with methanol to stop any enzymatic reaction, and analyzed subsequently by HPLC. The solvent systems were the following: solvent A: 0.1% (v/v) trifluoroacetic acid (TFA) in H_2O; solvent B: 0.095% (v/v) TFA in H_2O:CH_3CN 1:4; gradient elution from 10% to 70%B in 30 min, flow rate 1 mL min^{-1}, detection 215 nm. Retention factor (k') for each acceptor aldehyde and condensation product are given below.

NMR analysis: High-field ^{1}H and ^{13}C nuclear magnetic resonance (NMR) analyses were carried out at the Servei de Ressonància Magnètica Nuclear, Universitat Autònoma de Barcelona on an Avance 500 Bruker spectrometer for [D_6]DMSO, [D]CCl_3, and D_2O solutions. Full characterization of the described compounds was performed using typical gradient-enhanced two-dimensional experiments (COSY, NOESY, HSQC, and HMBC) recorded under routine conditions. When possible, NOE data was obtained from selective one-dimensional NOESY versions using a single pulsed-field-gradient echo as a selective excitation method and a mixing time of 500 ms. When necessary, proton and NOESY experiments were recorded at different temperatures in order to study the different behavior of the exchange phenomena to avoid the presence of false NOE cross-peaks that otherwise complicate both structural and dynamic studies. ^{1}H (300 MHz) and ^{13}C NMR (75 MHz) spectra were observed with a Unity-300 spectrometer from Varian (Palo Alto, California, USA) for [D_6]DMSO and [D]CCl_3 solutions and were carried out at the Instituto de Investigaciones Químicas y Ambientales-CSIC.

Elemental analyses and specific rotations: Elemental analyses were performed by the Servei de Microanàlisi Elemental IIQAB-CSIC. Specific rotations were measured with a Perkin–Elmer Model 341 (Überlingen, Germany) Polarimeter.

Molecular modeling: All molecular simulations were conducted with the program MOE (v. 2002.03, Chemical Computing Group, Montreal) using the implemented MMFF94 force field with its standard atomic charges and parameters. All energy calculations were carried out with the default parameters provided with the program, a distance-dependent dielectric

model for the electrostatic interactions, and a smoothed cut-off between 8 and 12 Å to model the nonbonded interactions. All minimizations were carried up to an RMS gradient < 0.01.

The coordinates for rabbit fructose-1,6-diphosphate aldolase covalently bound to reduced DHAP (rDHAP)[33] and for *E. coli* rhamnulose-1-phosphate aldolase complexed with phosphoglycolohydroxamic acid (PGH)[49] were obtained from the Protein Data Bank[50] at Brookhaven National Laboratory (entries 1J4E and 1GT7, respectively). The 1J4E structure is a homotetramer while the 1GT7 structure contains five homotetramers in the asymmetric unit. In addition, the 1J4E structure contains four Ala residues at positions 72, 239, 289, and 338 instead of the Cys residues found in the wild-type enzyme.[33] The simulations on RAMA were performed with chain A of 1J4E, after removing all water molecules, adding all the hydrogen atoms, and mutating the mentioned four Ala residues back to cysteine. The conformation of the side chains of these Cys residues was determined by minimization keeping the backbone coordinates fixed. Residues 1–3 and 345–363 were missing in the crystal structure and, therefore, they were not included in the simulations. The covalently bound rDHAP moiety was modified within MOE to convert it into the ligand shown in state II of Scheme 2. The conformational space of this intermediate was explored to find low-energy minima by running a stochastic conformational search keeping the coordinates of the protein fixed, except for the side chain of Lys229, and residues Asp33 and Lys229 charged as shown in Scheme 2. All conformations within 10 kcal mol^{-1} of the global minimum were kept and further minimized; this allowed motion of all protein residues that contained at least one atom within 12 Å from the bound ligand. The lowest-energy minimum found in this way was considered the global minimum. The structure of this ligand was further modified to generate the situation previous to the C–C bond formation, represented by state I in Scheme 2, in which the Cbz-alaninal molecule is close to the enamine bound to Lys229. To avoid that, the aldehyde molecule was removed away from this enamine and a restraint was imposed between the two carbon atoms that participate in the C–C bond formation (designated with an asterisk in state I of Scheme 2). This restraint was arbitrarily set to keep the distance between those two carbon atoms close to 2.5 Å. The conformational space of Cbz-alaninal was then stochastically searched as before, keeping the coordinates of the rest of the atoms fixed. Again, the conformations obtained were further minimized and the geometry of the global lowest-energy minimum determined.

For the simulations on RhuA we used chains A and B of 1GT7, since the active center of RhuA is located at the interface between two monomeric units of the protein. The PGH molecule was modified conveniently to obtain the α-hydroxyketonic ligand complexed to the Zn^{2+} ion as shown in state IV of Scheme 2. After finding the global minimum in the same way as before, this bound ligand was modified to generate the state before the C–C bond formation (state III, Scheme 2). The conformational space was searched again imposing a restraint to keep the distance between the two reactive carbon atoms close to 2.5 Å.

In all cases the RMSD calculated for the residues of the protein that were allowed to relax during the minimization was between 0.6 and 1 Å relative to the conformation of the same residues in the crystallographic structures.

Synthesis of *N*-protected amino alcohols

Cbz-amino alcohols: Cbz-OSu (11–56 mmol) in dioxane/water 4:1 (10–50 mL) was added to a solution of the aminoalcohol (13–67 mmol) in dioxane/water 4:1 (50–150 mL). After stirring for 12 h, the mixture was evaporated to dryness under reduced pressure. The residue was dissolved with ethyl acetate and washed successively with citric acid 5% (w/v) ($3\times$ 50–75 mL), $NaHCO_3$ 10% (w/v) (3×50–75 mL), and brine (3×50–75 mL). After drying over Na_2SO_4, the organic layer was evaporated under reduced pressure. NMR spectrum and HPLC analysis of the residue showed only one product.

Benzyl 3-hydroxypropylcarbamate (1): The title compound (9.6 g) was obtained in 82% yield by using the above general procedure. M.p. 48–52 °C.

Benzyl 2-hydroxyethylcarbamate (Cbz-glycinol) (2): The title compound (8.9 g) was obtained in 89% yield by using the above general procedure. M.p. 57–63 °C.

(*S*)-Benzyl-2-hydroxy-1-methylethylcarbamate ((*S*)-Cbz-L-alaninol) (3): The title compound (7.9 g) was obtained in 90% yield by using the above general procedure. M.p. 82–84 °C; the m.p. and ^{1}H and ^{13}C NMR spectra of these products were consistent with those reported in the literature.[51–53]

(*R*)-Benzyl-2-hydroxy-1-methylethylcarbamate ((*R*)-Cbz-D-alaninol) (4): The title compound (2.0 g) was obtained in 86% yield by using the above general procedure. M.p. 82–84 °C; ^{1}H NMR (200 MHz, [D]CCl_3, 25 °C): $\delta = 7.2$ (m, 5H; Ph), 5.1 (s, 2H; CH_2Ph), 5.0 (br, 1H; NH), 3.9 (m, 1H; NHC*H*), 3.7 (m, 1H; CH_2OH), 3.5 (m, 1H; CH_2OH), 1.2 ppm (d, 3H; CH_3); ^{13}C NMR: $\delta = 136.0$ (quat. C), 128.5, 128.1, 128.0 (CH, Ph), 156.5 (OCONH), 66.8 (CH_2OH + CH_2Ph), 48.9 (CH), 17.2 ppm (CH_3).

Synthesis of *N*-protected aminoaldehydes: The synthesis of *N*-protected aminoaldehydes was achieved by oxidation of the corresponding *N*-protected aminoalcohols. Two oxidation procedures were used as described below.

Swern oxidation with slight modifications according to Konradi et al.:[54] A solution of dimethylsulfoxide (7.7–18 mmol) in dried dichloromethane (2–4 mL) was added dropwise under argon to a cooled solution (−65 °C) of oxalyl chloride (7.7–18 mmol) in dried methylene chloride (2–4 mL). After stirring for 10 min, a solution of the Cbz-aminoalcohol (5.2–12 mmol) in dried methylene chloride (4 mL) was added slowly whilst maintaining the temperature at −65 °C. The solution was stirred for 45 min at −65 °C and then triethylamine (51 mmol) was added dropwise. After being stirred for an additional 10 min at −65 °C, cold ethyl acetate (50–100 mL) and cold brine solution (25–50 mL) were added. The organic layer was washed with brine solution (3×50–100 mL), dried over Na_2SO_4, and evaporated to dryness under reduced pressure. The residue was further purified by crystallization or by preparative HPLC methodology.

Benzyl 3-oxoproylcarbamate (5):[52] The title compound (2.1 g, 84% yield) was prepared according to the general procedure above. HPLC: $k' = 8.7$; m.p. 55–57 °C; ^{1}H NMR (300 MHz, [D]CCl_3, 25 °C): $\delta = 9.7$ (s, 1H; CHO), 7.2 (m, 5H; Ph), 5.2 (s, 1H; NH), 5.0 (s, 2H; CH_2O), 3.3 (q, 2H; NHCH_2), 2.6 ppm (t, 2H; CH_2CHO); ^{13}C NMR (75 MHz, $CDCl_3$, 25 °C): $\delta = 201.0$ (CHO), 157.0 (CONH), 136.0 (quat. C), 128.5, 128.1, 128.0 (CH, Ph), 66.7 (CH_2Ph), 44.0 ($NHCH_2$), 34.5 ppm (CH_2CHO).

Benzyl 2-oxoethylcarbamate (Cbz-glycinal) (6): The reaction workup provided an oil (1.9 g, 95% yield, 85% pure by HPLC), which was further purified by reversed-phase HPLC. The oil (1.9 g) was dissolved in DMSO, loaded onto the preparative PrePack cartridge (47×300 mm) filled with a Bondapack C18, 300 Å, 15–20 μm stationary phase, and eluted with a CH_3CN gradient (0 to 20% in 30 min) in plain water. The flow rate was 100 mL min^{-1} and the products were detected at either 215 or 225 nm. Analysis of the fractions was accomplished by analytical RP chromatography using the same elution conditions, flow rate, and detection as previously described. Pure fractions were pooled and lyophilized to yield **6** (0.65 g, 33% overall yield, 99.9% pure by HPLC) as an oil. ^{1}H NMR data are consistent with those reported in the literature;[55] HPLC: $k' = 7.6$; ^{13}C NMR (75 MHz, [D_6]DMSO, 25 °C): $\delta = 200.2$ (CHO), 156.6 (CONH), 136.9 (quat. C), 128.4, 128.3, 127.8 (CH, Ph), 65.5 (CH_2O), 50.6 ppm (CH_2CHO).

(*S*)-Benzyl 1-methyl-2-oxoethylcarbamate ((*S*)-Cbz-alaninal) (7): The title compound (0.45 g, 90% yield) was obtained as a pale yellow oil by using the general procedure above. HPLC: $k' = 8.8$; $[\alpha]_D^{20} = -16.3$ ($c = 1$ in MeOH); ^{1}H NMR (300 MHz, [D_6]DMSO, 25 °C): $\delta = 9.5$ (1H, s, CHO), 5.0 (2H, s; CH_2O), 4.0 (1H, m; CH), 1.2 ppm (3H, d; CH_3); ^{13}C NMR (75 MHz, [D_6]DMSO, 25 °C): $\delta = 201$ (CHO), 156.1 (CONH), 65.7 (CH_2O), 55.1 (CH), 13.8 ppm (CH_3).

Oxidation with 2-iodoxybenzoic acid (IBX): 2-Iodoxybenzoic acid was prepared as described in the literature.[24, 56] ***Caution!*** IBX has been reported to detonate upon heavy impact and/or heating over 200 °C.

(*S*)-Benzyl 1-methyl-2-oxoethylcarbamate ((*S*)-Cbz-alaninal) (7): IBX (24-48 mmol) was added to a solution of (*S*)-Cbz-alaninol (10–19 mmol) in DMSO (60–120 mL). The reaction was monitored by HPLC until no alcohol was detected. At this point, the reaction mixture was diluted with water (30–60 mL) and the mixture was extracted with ethyl acetate ($3\times$ 75–100 mL). The organic layers were pooled, washed with $NaHCO_3$ 5% (w/w) (3×100 mL) and brine (3×100 mL), dried over Na_2SO_4, and evaporated under reduced pressure to give the title compound (2.5 g, 63% yield) as a colorless oil. HPLC: $k' = 8.8$; $[\alpha]_D^{20} = -19.9$ ($c = 1$ in MeOH); ^{1}H NMR and ^{13}C NMR were identical to those described above.

(*R*)-Benzyl 1-methyl-2-oxoethylcarbamate ((*R*)-Cbz-alaninal) (8): The title compound (1.4 g, 74% yield) was obtained as a colorless oil by using

the procedure described above except starting from (*R*)-Cbz-alaninol. HPLC: $k' = 8.8$; $[\alpha]_D^{20} = 18.7$ ($c = 1$ in MeOH); ^{1}H NMR (300 MHz, [D$_6$]DMSO, 25 °C): $\delta = 9.5$ (s, 1H; CHO), 5.0 (s, 2H; CH$_2$O), 4.0 (m, 1H; CH), 1.2 ppm (d, 3H; CH$_3$); ^{13}C NMR (75 MHz, [D$_6$]DMSO, 25 °C): $\delta =$ 201.0 (CHO), 156.1 (CONH), 65.7 (CH$_2$O), 55.1 (CH), 13.8 ppm (CH$_3$).

Enzymatic reactions in emulsions: Reactions were carried out in 10-mL test tubes with screw caps. The aldehyde (0.125, 0.5, or 0.9 mmol), the oil (6% w/w), and the surfactant (4% w/w) were mixed vigorously. Then, the DHAP solution (0.075–0.3 mmol) at pH 6.9, freshly prepared as described by Effenberger et al.,[57] was added dropwise while stirring at 25 °C with a vortex mixer. A reaction volume of 2.5 mL or 5 mL was employed for analytical or preparative scale, respectively. Finally, RAMA (0.65–4 mg giving 0.26–1.6 mg g^{-1} in the final reaction mixture, 19.5 U mg^{-1}) or RhuA (20–40 μL giving 4–16 μL mL^{-1} in the final reaction mixture, 100 U mL^{-1}) was added and mixed again. The test tubes were placed on a horizontal shaking bath (100 rpm) at constant temperature (25 °C). The reactions were followed by HPLC until the peak of the product reached a maximum. The enzymatic reactions were stopped by addition of MeOH, and the final crude purified as described above. The reactions at semipreparative level were scale up proportionally to a total reaction volume of 5 mL.

Enzymatic reactions in mixtures dimethylformamide/water 1:4: Reactions were carried out in 10-mL test tubes with screw caps. The aldehyde (0.125–0.36 mmol) was dissolved in DMF 20% (v/v). Then, the DHAP solution (0.075–0.225 mmol), prepared as described above, was added dropwise while mixing. The rest of the experimental procedure was identical to that described for the reaction in emulsions.

Purification procedures: The condensation products were purified by ion-exchange chromatography on an FPLC system taking advantage of the phosphate group. Bulk stationary phase MacroPrep High Q Support, 50 μm strong anion-exchange resin in neutral form, Cl$^-$ as counter ion, was packed into a glass Pharmacia FPLC (Uppsala, Sweden) C26/40-type column to a final bed volume of 40 mL. The flow rate was 3 mL min^{-1}, 0.1 MPa. The resin was equilibrated initially with EtOH/H$_2$O (3:2). Aliquots of the crude reaction mixture were loaded onto the column and the excess aldehyde and neutral and cationic impurities were eliminated by washing with EtOH/H$_2$O (3:2). Then the target product was eluted with 250 mM NaCl in EtOH/H$_2$O (3:2). The operation was repeated until the whole crude was consumed. Fractions containing the pure product were pooled and evaporated to dryness under reduced pressure. The residue was dissolved in water and desalted by reversed-phase HPLC on a Perkin–Elmer semipreparative 250 × 25 mm column, filled with C18, 5 μm-type stationary phase by using the following procedure: first, the column was equilibrated with 0.1% (v/v) TFA in water. The sample was then adjusted to pH 3–4 with TFA and loaded onto the column. First, the salt was eliminated by washing with 0.1% (v/v) TFA in water (100 mL) and then with plain water (50 mL) to eliminate the acid. Then, the product was eluted with a gradient elution of CH$_3$CN (0 to 48% v/v in 30 min) in plain water. The flow rate was 10 mL min^{-1} and the products were detected at 225 nm. The pure fractions were pooled, the excess CH$_3$CN was evaporated under reduced pressure, the pH of the resulting aqueous solution was adjusted to 7 with NaOH and finally lyophilized.

Physical and spectral data of the linear compounds linear compounds 9–16: The melting points of the compounds given below correspond to lyophilized solids rather than crystals. Note that some of them are mixtures of epimers at C-4. The yields correspond to the amounts obtained from the aldol enzymatic reactions at semipreparative level. The purification procedures were not optimized.

(3*S*)-6-{[(Benzyloxy)carbonyl]amino}-5,6-dideoxy-1-*O*-phosphonohex-2-ulose sodium salt (9): The title compound (540 mg) was obtained in 40% yield. HPLC: $k' = 5.2$; m.p. 109–111 °C; ^{1}H NMR (500 MHz, D$_2$O, 25 °C) major diastereoisomer: $\delta = 7.2$ (m, 5H; Ph), 4.9 (s, 2H; PhC*H*$_2$), 4.6 (dd, ^3J(H,H) = 6.3 Hz, ^3J(H,H) = 18.6 Hz, 1H; C*H*$_2$OP), 4.5 (dd, ^3J(H,H) = 7.0 Hz, ^3J(H,H) = 18.6 Hz, 1H; CH$_2$OP), 4.25 (s, 1H; C*H*OH), 4.0 (t, 1H; C*H*OH), 3.1 (m, 2H; NHC*H*$_2$), 1.6 ppm (m, 2H; C*H*$_2$CHOH); minor diastereoisomer: $\delta = 7.2$ (m, 5H, Ph), 5.0 (s, 2H; PhCH$_2$), 4.27 (1H; C*H*OH), 3.82 (1H; C*H*OH), 3.1 (m, 2H; NHC*H*$_2$), 1.5 ppm (m, 2H; C*H*$_2$CHOH); cyclic product: $\delta = 3.8$ (1H; C*H*$_2$OP), 3.65 ppm (1H; C*H*$_2$OP); ^{13}C NMR (125 MHz, D$_2$O, 25 °C) major diastereoisomer: $\delta =$ 210.8, (C2), 158.2 (C7), 136.4, 128.0 (Ar), 78.4 (C3), 69.1 (C4), 68.4 (C1), 67.2 (C8), 37.4 (C6), 33.0 ppm (C5); elemental analysis calcd (%) for C$_{14}$H$_{18}$NO$_9$Na$_2$P · 2H$_2$O: C 36.77, H 4.85, N 3.06; found: C 36.59, H 4.94, N 3.04.

(3*S*)-5-{[(Benzyloxy)carbonyl]amino}-5-deoxy-1-*O*-phosphonopent-2-ulose sodium salt (10): The title compound (416 mg) was obtained in 50% yield. HPLC: $k' = 4.1$; m.p. 114–118 °C; ^{1}H NMR (500 MHz, D$_2$O, 12 °C) linear product: $\delta = 7.2$ (m, 5H; Ph), 4.9 (s, 2H; PhC*H*$_2$), 4.5 (dd, ^3J(H,H) = 6.3 Hz, ^3J(H,H) = 18.7 Hz, 2H; C*H*$_2$OP), 4.3 (d, $^3J_{3,4}$(H,H) = 1.8, 1H; C*H*OH), 4.0 (dt, $^3J_{4,5}$(H,H) = 5.8 Hz, $^3J_{4,5'}$(H,H) = 7.7 Hz, 1H; C*H*OH), 3.1 (dd, 1H, $^3J_{5,5'}$(H,H) = 13.8 Hz, 1H; NHC*H*$_2$), 3.0 ppm (dd, 1H; NHC*H*$_2$); cyclic species, conformer I: $\delta = 7.2$ (m, 5H; Ph), 4.9 (s, 2H; PhC*H*$_2$), 4.1 (d, 1H; C*H*OH), 4.1 (d, 1H; C*H*$_2$OP), 3.9 (dd, 1H; C*H*OH), 3.8 (dd, 1H; NHC*H*$_2$), 3.6 (d, 1H; C*H*$_2$OP), 2.9 ppm (t, 1H; NHC*H*$_2$); cyclic species, conformer II: $\delta = 5.0$ (s, 2H; PhC*H*$_2$), 4.1 (d, 1H; C*H*OH), 3.9 (d, 1H; C*H*$_2$OP), 3.9 (dd, 1H; C*H*OH), 3.8 (dd, 1H; NHC*H*$_2$), 3.5 (d, 1H; C*H*$_2$OP), 2.8 ppm (t, 1H; NHC*H*$_2$); ^{13}C NMR (125 MHz, D$_2$O, 12 °C): $\delta = 210.8$ (C2), 158.7 (C6), 136.4 (Ar), 127.9 (Ar), 75.6 (C3), 69.4 (C4), 67.4 (C7), 67.6 (C1), 41.9 ppm (C5); elemental analysis calcd (%) for C$_{13}$H$_{16}$NO$_9$Na$_2$P · 2H$_2$O: C 35.23, H 4.55, N 3.16; found: C 35.24, H 4.47, N 3.07.

(3*S*,5*S*)-5-{[(Benzyloxy)carbonyl]amino}-5,6-dideoxy-1-*O*-phosphonohex-2-ulose sodium salt (11): The title compound (33 mg) was obtained in 10% yield. HPLC: $k' = 4.5$; m.p. 117–120 °C; elemental analysis calcd (%) for C$_{14}$H$_{18}$NO$_9$Na$_2$P · ½H$_2$O: C 37.48, H 4.68, N 3.12; found: C 37.41, H 4.82, N 3.06.

(3*S*,5*R*)-5-{[(Benzyloxy)carbonyl]amino}-5,6-dideoxy-1-*O*-phosphonohex-2-ulose sodium salt (12): The title compound (230 mg) was obtained in 46% yield. HPLC: $k' = 4.5$, m.p. 119–123 °C; elemental analysis calcd (%) for C$_{14}$H$_{18}$NO$_9$Na$_2$P · ½H$_2$O · NaCl: C 36.05, H 4.29, N 3.00; found: C 36.15, H 4.61; N 2.98.

(3*R*)-6-{[(Benzyloxy)carbonyl]amino}-5,6-dideoxy-1-*O*-phosphonohex-2-ulose sodium salt (13): The title compound (330 mg) was obtained in 40% yield. HPLC: $k' = 5.2$, m.p. 109–111 °C; elemental analysis calcd (%) for C$_{14}$H$_{18}$NO$_9$Na$_2$P · 3H$_2$O: C 35.38, H 5.09, N 2.95; found: C 35.55, H 5.04, N 3.01.

(3*R*)-5-{[(Benzyloxy)carbonyl]amino}-5-deoxy-1-*O*-phosphonopent-2-ulose sodium salt (14): The title compound (229 mg) was obtained in 53% yield. HPLC: $k' = 4.1$, m.p. 114–118 °C; elemental analysis calcd (%) for: C$_{13}$H$_{16}$NO$_9$Na$_2$P · ½H$_2$O: C 35.93, H 4.38, N 3.22; found: C 35.95, H 4.24, N 3.20.

(3*R*,5S)-5-{[(Benzyloxy)carbonyl]amino}-5,6-dideoxy-1-*O*-phosphonohex-2-ulose sodium salt (15): The title compound (158 mg) was obtained in 35% yield. HPLC: $k' = 4.9$, m.p. 132–136 °C; elemental analysis calcd (%) for: C$_{14}$H$_{18}$NO$_9$Na$_2$P · 3H$_2$O: C 35.38, H 5.09, N 2.95; found: C 35.13, H 4.95, N 2.95.

(3*R*,5*R*)-5-{[(Benzyloxy)carbonyl]amino}-5,6-dideoxy-1-*O*-phosphono-hex-2-ulose sodium salt (16): The title compound (255 mg) was obtained in 45% yield. HPLC: $k' = 4.5$, m.p. 130–132 °C; elemental analysis calcd (%) for: C$_{14}$H$_{18}$NO$_9$Na$_2$P · ½H$_2$O: C 37.48, H 4.68, N 3.12; found: C 37.34, H 4.70, N 3.03.

Removal of phosphate groups and catalytic hydrogenation: The phosphate group of compounds **9–16** was removed by hydrolysis catalyzed by acid phosphatase following the procedure described by Bednarski et al.[27] The reaction was followed by HPLC until no starting material was detected. Then the crude was desalted by HPLC and lyophilized. The residue was dissolved in methanol and the solution hydrogenated under 50 psi H$_2$ for 24 h with Pd/C as catalyst. The reaction mixture was then filtered through neutral alumina, the solvent removed under reduced pressure, the residue dissolved in plain water, adjusted to pH 6.5 and lyophilized.

(2*R*,3*R*,4*R*)-2-(Hydroxymethyl)piperidine-3,4-diol (17) and (2*S*,3*R*,4*S*)-2-(hydroxymethyl)piperidine-3,4-diol (18): The title compounds were prepared according to the general procedure described above. ^{1}H NMR (500 MHz, D$_2$O, 25 °C) major **17**: $\delta = 3.84$ (dd, ^3J(H,H) = 3.2 Hz, ^3J(H,H) = 12.6 Hz, 1H; H7), 3.77 (dd, ^3J(H,H) = 5.7 Hz, ^3J(H,H) = 12.7 Hz, 1H; H7), 3.6 (dt, ^3J(H,H) = 4.9 Hz, ^3J(H,H) = 9.5 Hz, ^3J(H,H) = 11.6, 1H; H4), 3.4 (t, 1H; H3), 3.3 (br, 1H; H6), 3.0 (m, 1H; H2), 2.95 (dt, ^3J(H,H) = 3.2 Hz, ^3J(H,H) = 13.1 Hz, 1H; H6), 2.1 (br, 1H, H5), 1.6 ppm (dq, ^3J(H,H) = 4.3 Hz, 1H; H5); minor **18**: $\delta = 4.0$ (1H; H3), 3.80 (1H; H4), 3.2 (1H; H2), 1.95 (1H; H5), 1.85 (1H; H5), 3.76 (dd, 1H; H7), 3.72 (dd, 1H; H7), 2.95 (1H; H6), 3.0 ppm (1H; H6); ^{13}C NMR (125 MHz, D$_2$O, 25 °C) major **17**: $\delta = 70.5$ (C4), 69.7 (C3), 60.0 (C2), 57.9 (C7), 41.7 (C6), 28.8 ppm (C5);

minor **18**: $\delta = 67.6$ (C4), 66.2 (C3), 60.3 (C2), 59.9 (C7), 42.2 (C6), 24.5 ppm (C5).

(2*R*,3*R*,4*R*)-2-(Hydroxymethyl)pyrrolidine-3,4-diol (19): The title compound was prepared according to the general procedure described above. ^{1}H NMR (500 MHz, D_2O, 25 °C): $\delta = 4.2$ (m, $^3J(H,H) = 2.8$ Hz, $^3J(H,H) = 3.9$ Hz, $^3J(H,H) = 5.0$ Hz, 1H; H4), 3.9 (t, $^3J(H,H) = 3.9$ Hz, 1H; H3), 3.8 (dd, $^3J(H,H) = 4.9$ Hz, $^3J(H,H) = 11.9$ Hz, 1H; H6), 3.7 (dd, $^3J(H,H) = 7.0$ Hz, $^3J(H,H) = 11.9$ Hz, 1H; H6), 3.4 (dd, $^3J(H,H) = 5.0$ Hz, $^3J(H,H) = 12.3$ Hz, 1H; H5), 3.3 (m, $^3J(H,H) = 3.9$ Hz, $^3J(H,H) = 4.9$ Hz, $^3J(H,H) = 7.3$ Hz, 1H; H2), 3.1 ppm (dd, $^3J(H,H) = 2.8$ Hz, $^3J(H,H) = 12.3$ Hz, 1H; H5); ^{13}C NMR (125 MHz, D_2O): $\delta = 76.5$ (C3), 75.1 (C4), 66.6 (C2), 59.7 (C6), 50.2 ppm (C5).

(2*R*,3*R*,4*R*,5*S*)-2-Hydroxymethyl-5-methylpyrrolidine-3,4-diol (20): The title compound was prepared according to the general procedure described above. ^{1}H NMR (500 MHz, D_2O, 25 °C): $\delta = 4.1$ (dd, $^3J(H,H) = 1.4$ Hz, $^3J(H,H) = 3.2$ Hz, 1H; H4), 4.0 (dd, $^3J(H,H) = 1.8$, $^3J(H,H) = 3.2$, 1H; H3), 3.8 (dd, $^3J(H,H) = 4.9$ Hz, $^3J(H,H) = 11.9$ Hz, 1H; H7), 3.75 (dq, $^3J(H,H) = 3.5$ Hz, $^3J(H,H) = 6.5$ Hz, 1H; H5), 3.7 (dd, $^3J(H,H) = 8.8$ Hz, $^3J(H,H) = 12.3$ Hz, 1H; H7), 3.5 (dt, $^3J(H,H) = 3.3$ Hz, $^3J(H,H) = 5.1$ Hz, $^3J(H,H) = 8.2$ Hz, 1H; H2), 1.3 ppm (d, $^3J(H,H) = 6.7$ Hz, 3H; H6); ^{13}C NMR (125 MHz, D_2O, 25 °C): $\delta = 76.3$ (C4), 76.3 (C3), 67.5 (C2), 59.6 (C7), 58.3 (C5), 10.7 ppm (C6).

(2*R*,3*R*,4*R*,5*R*)-2-Hydroxymethyl-5-methylpyrrolidine-3,4-diol (21): The title compound was prepared according to the general procedure described above. ^{1}H NMR (500 MHz, D_2O, 25 °C): $\delta = 3.9$ (t, $^3J(H,H) = 7$ Hz, 1H; H3), 3.8 (dd, $^3J(H,H) = 4.2$ Hz, $^3J(H,H) = 12.0$ Hz, 1H; H7), 3.75 (t, $^3J(H,H) = 7.5$ Hz, 1H; H4), 3.7 (dd, $^3J(H,H) = 6.4$ Hz, $^3J(H,H) = 12.0$ Hz, 1H; H7), 3.35 (dt, $^3J(H,H) = 4.2$ Hz, $^3J(H,H) = 6.4$ Hz, $^3J(H,H) = 7.0$ Hz, 1H; H2), 3.3 (dq, $^3J(H,H) = 7.0$ Hz, 1H; H5), 1.3 ppm (d, $^3J(H,H) = 7.0$ Hz, 3H; H6); ^{13}C NMR (75 MHz, D_2O, 25 °C): $\delta = 80.3$ (C4), 75.8 (C3), 62.4 (C2), 59.6 (C7), 57.3 (C5), 15.4 ppm (C6).

(2*S*,3*S*,4*S*)-2-(Hydroxymethyl)piperidine-3,4-diol (22) and (2*R*,3*S*,4*R*)-2-(hydroxymethyl)piperidine-3,4-diol (23): The title compounds were prepared according to the general procedure described above. ^{1}H NMR (500 MHz, D_2O, 25 °C) major **22**: $\delta = 3.84$ (dd, $^3J(H,H) = 3.2$, $^3J(H,H) = 12.6$ Hz, 1H; H7), 3.77 (dd, $^3J(H,H) = 5.7$ Hz, $^3J(H,H) = 12.7$ Hz, 1H; H7), 3.6 (dt, $^3J(H,H) = 4.9$ Hz, $^3J(H,H) = 9.5$ Hz, $^3J(H,H) = 11.6$ Hz, 1H; H4), 3.4 (t, 1H; H3), 3.3 (br, 1H; H6), 3.0 (m, 1H; H2), 2.95 (dt, $^3J(H,H) = 3.2$ Hz, $^3J(H,H) = 13.1$ Hz, 1H; H6), 2.1 (br, 1H; H5), 1.6 ppm (dq, $^3J(H,H) = 4.3$ Hz, 1H; H5); minor **23**: $\delta = 4.0$ (1H; H3), 3.80 (1H; H4), 3.2 (1H; H2), 1.95 (1H; H5), 1.85 (1H; H5), 3.76 (dd, 1H; H7), 3.72 (dd, 1H; H7), 2.95 (1H; H6), 3.0 ppm (1H; H6); ^{13}C NMR (125 MHz, D_2O, 25 °C) major **22**: $\delta = 70.5$ (C4), 69.7 (C3), 60.0 (C2), 57.9 (C7), 41.7 (C6), 28.8 ppm (C5); minor **23**: $\delta = 67.6$ (C4), 66.2 (C3), 60.3 (C2), 59.9 (C7), 42.2 (C6), 24.5 ppm (C5).

(2*S*,3*S*,4*S*)-2-(Hydroxymethyl)pyrrolidine-3,4-diol (24) and (2*R*,3*S*,4*R*)-2-(hydroxymethyl)pyrrolidine-3,4-diol (25): The title compounds were prepared according to the general procedure described above. ^{1}H NMR (500 MHz, D_2O, 25 °C) major **24**: $\delta = 4.2$ (m, $^3J(H,H) = 2.8$, $^3J(H,H) = 3.9$ Hz, $^3J(H,H) = 5.0$ Hz, 1H; H4), 3.9 (t, $^3J(H,H) = 3.9$ Hz, 1H; H3), 3.8 (dd, $^3J(H,H) = 4.9$ Hz, $^3J(H,H) = 11.9$ Hz, 1H; H6), 3.7 (dd, $^3J(H,H) = 7.0$ Hz, $^3J(H,H) = 11.9$ Hz, 1H; H6), 3.4 (dd, $^3J(H,H) = 5.0$ Hz, $^3J(H,H) = 12.3$ Hz, 1H; H5), 3.3 (m, $^3J(H,H) = 3.9$ Hz, $^3J(H,H) = 4.9$ Hz, $^3J(H,H) = 7.3$ Hz, 1H; H2), 3.1 ppm (dd, $^3J(H,H) = 2.8$ Hz, $^3J(H,H) = 12.3$ Hz, 1H; H5); minor **25**: $\delta = 4.4$ (dt, $^3J(H,H) = 3.8$ Hz, $^3J(H,H) = 4.3$ Hz, $^3J(H,H) = 7.3$ Hz, 1H; H4), 4.2 (t, 1H; H3), 3.9 (dd, $^3J(H,H) = 4.9$ Hz, $^3J(H,H) = 12.0$ Hz, 1H; H6), 3.8 (dd, $^3J(H,H) = 6.6$ Hz, $^3J(H,H) = 12.3$ Hz, 1H; H6), 3.6 (m, 1H; H2), 3.3 (dd, $^3J(H,H) = 4.3$ Hz, $^3J(H,H) = 12.0$ Hz, 1H; H5), 3.4 ppm (dd, $^3J(H,H) = 7.3$ Hz, $^3J(H,H) = 12.3$ Hz, 1H; H5); ^{13}C NMR (125 MHz, D_2O, 25 °C) major **24**: $\delta = 76.5$ (C3), 75.1 (C4), 66.6 (C2), 59.7 (C6), 50.2 ppm (C5); minor **25**: $\delta = 70.5$ (C3), 70.7 (C4), 63.2 (C2), 58.4 (C6), 47.9 ppm (C5).

(2*S*,3*S*,4*S*,5*S*)-2-Hydroxymethyl-5-methylpyrrolidine-3,4-diol (26): The title compound was prepared according to the general procedure described above. ^{1}H NMR (500 MHz, D_2O, 25 °C): $\delta = 3.9$ (t, $^3J(H,H) = 7.0$ Hz, 1H; H3), 3.8 (dd, $^3J(H,H) = 4.2$ Hz, $^3J(H,H) = 12.0$ Hz, 1H; H7), 3.75 (t, $^3J(H,H) = 7.5$ Hz, 1H; H4), 3.7 (dd, $^3J(H,H) = 6.4$ Hz, $^3J(H,H) = 12.0$ Hz, 1H; H7), 3.35 (dt, $^3J(H,H) = 4.2$ Hz, $^3J(H,H) = 6.4$ Hz, $^3J(H,H) = 7.0$ Hz, 1H; H2), 3.3 (dq, $^3J(H,H) = 7.0$ Hz, 1H; H5), 1.3 ppm (d, $^3J(H,H) = 7.0$ Hz, 3H; H6); ^{13}C NMR (125 MHz, D_2O, 25 °C): $\delta = 80.3$ (C4), 75.8 (C3), 62.4 (C2), 59.6 (C7), 57.3 (C5), 15.4 ppm (C6).

(2*S*,3*S*,4*S*,5*R*)-2-Hydroxymethyl-5-methylpyrrolidine-3,4-diol (27) and (2*R*,3*S*,4*R*,5*R*)-2-hydroxymethyl-5-methylpyrrolidine-3,4-diol (28): The title compounds were prepared according to the general procedure described above. ^{1}H NMR (500 MHz, D_2O, 25 °C) major **27**: $\delta = 4.1$ (dd, $^3J(H,H) = 1.4$ Hz, $^3J(H,H) = 3.2$ Hz, 1H; H4), 4.0 (dd, $^3J(H,H) = 1.8$ Hz, $^3J(H,H) = 3.2$ Hz, 1H; H3), 3.8 (dd, $^3J(H,H) = 4.9$ Hz, $^3J(H,H) = 11.9$ Hz, 1H; H7), 3.75 (dq, $^3J(H,H) = 3.5$ Hz, $^3J(H,H) = 6.5$ Hz, 1H; H5), 3.7 (dd, $^3J(H,H) = 8.8$ Hz, $^3J(H,H) = 12.3$ Hz, 1H; H7), 3.5 (dt, $^3J(H,H) = 3.3$ Hz, $^3J(H,H) = 5.1$ Hz, $^3J(H,H) = 8.2$ Hz, 1H; H2), 1.3 ppm (d, $^3J(H,H) = 6.7$ Hz, 3H; H6); minor **28**: $\delta = 4.3$ (t, $^3J(H,H) = 3.7$ Hz, 1H; H3), 3.95 (dd, $^3J(H,H) = 3.7$ Hz, $^3J(H,H) = 9$ Hz, 1H; H4), 3.9 (dd, $^3J(H,H) = 4.7$ Hz, $^3J(H,H) = 11.8$ Hz, 1H; H7), 3.8 (dd, $^3J(H,H) = 8.4$ Hz, $^3J(H,H) = 11.8$ Hz, 1H; H7), 3.75 (m, $^3J(H,H) = 3.7$ Hz, $^3J(H,H) = 4.7$ Hz, $^3J(H,H) = 8.4$ Hz, 1H; H2), 3.5 (m, 1H; H5), 1.3 ppm (d, $^3J(H,H) = 6.7$ Hz, 3H; H6); ^{13}C NMR (125 MHz, D_2O, 25 °C) major **27**: $\delta = 76.3$ (C4), 76.3 (C3), 67.5 (C2), 59.6 (C7), 58.3 (C5), 10.7 ppm (C6); minor **28**: $\delta = 76.7$ (C4), 70.4 (C3), 61.5 (C2), 58.4 (C7), 56.7 (C5), 15.0 ppm (C6).

Acknowledgement

Financial support from the Spanish M.C.Y.T. Plan Nacional (grants QUI99-0997CO2-01, BIO99-1219-C02-02 and PPQ2002-04625-C02-01) and from Generalitat de Catalunya (grant 2000SGR-00357) is acknowledged.

[1] T. D. Machajewski, C. H. Wong, *Angew. Chem.* **2000**, 112, 1406 – 1430; *Angew. Chem. Int. Ed.* **2000**, *39*, 1353 – 1374.
[2] W. D. Fessner, V. Helaine, *Curr. Opin. Biotechnol.* **2001**, *12*, 574 – 586.
[3] C.-H. Wong, R. L. Halcomb, Y. Ichikawa, T. Kajimoto, *Angew. Chem.* **1995**, 107, 453 – 474; *Angew. Chem. Int. Ed. Engl.* **1995**, *34*, 412 – 432.
[4] G. C. Look, C. H. Fotsch, C. H. Wong, *Acc. Chem. Res.* **1993**, *26*, 182 – 190.
[5] C. H. Wong, *Trends Biotechnol.* **1992**, *10*, 337 – 341.
[6] S. Takayama, R. Martin, J. Wu, K. Laslo, G. Siuzdak, C.-H. Wong, *J. Am. Chem. Soc.* **1997**, *119*, 8146 – 8151.
[7] M. H. Fechter, A. E. Stutz, A. Tauss, *Curr. Org. Chem.* **1999**, *3*, 269 – 285.
[8] C.-H. Wong, L. Provencher, J. A. Porco, Jr., S.-H. Jung, Y.-F. Wang, L. Chen, R. Wang, D. H. Steensma, *J. Org. Chem.* **1995**, *60*, 1492 – 1501.
[9] A. E. Stutz, *Iminosugars as Glycosidase Inhibitors. Nojirimicin and Beyond*, Wiley-VCH, Weinheim, **1999**.
[10] V. H. Lillelund, H. H. Jensen, X. Liang, M. Bols, *Chem. Rev.* **2002**, *102*, 515 – 553.
[11] R. R. Hung, J. A. Straub, G. M. Whitesides, *J. Org. Chem.* **1991**, *56*, 3849 – 3855.
[12] J. Jurczak, A. Golebiowski, *Chem. Rev.* **1989**, *89*, 149 – 164.
[13] J. Jurczak, D. Gryko, E. Kobrzycka, H. Gruza, P. Prokopowicz, *Tetrahedron* **1998**, *54*, 6051 – 6064.
[14] M. Schuster, *Bioorg. Med. Chem. Lett.* **1999**, *9*, 615 – 618.
[15] C. H. Von der Osten, A. J. Sinskey, C. F. Barbas, III, R. L. Pederson, Y. F. Wang, C. H. Wong, *J. Am. Chem. Soc.* **1989**, *111*, 3924 – 3927.
[16] A. Romero, C. H. Wong, *J. Org. Chem.* **2000**, *65*, 8264 – 8268.
[17] R. L. Pederson, C. H. Wong, *Heterocycles* **1989**, *28*, 477 – 480.
[18] L. Azema, F. Bringaud, C. Blonski, J. Perie, *Bioorg. Med. Chem.* **2000**, *8*, 717 – 722.
[19] S. B. Sobolov, A. Bartoszko-Malik, T. R. Oeschger, M. M. Montelbano, *Tetrahedron Lett.* **1994**, *35*, 7751 – 7754.
[20] P. Clapés, L. Espelt, M. A. Navarro, C. Solans, *J. Chem. Soc. Perkin Trans. 2* **2001**, 1394 – 1399.
[21] L. Espelt, P. Clapés, J. Esquena, A. Manich, C. Solans, *Langmuir* **2003**, *19*, 1337 – 1346.
[22] C. Solans, R. Pons, H. Kunieda, in *Modern Aspects of Emulsion Science* (Ed.: B. P. Binks), The Royal Society of Chemistry, Cambridge, **1998**, pp. 367 – 394.
[23] Swern oxidation of alcohol **3** furnished **7** with lower optical purity than that obtained with IBX.
[24] M. Frigerio, M. Santagostino, S. Sputore, *J. Org. Chem.* **1999**, *64*, 4537 – 4538.

[25] A. G. Myers, B. Zhong, M. Movassaghi, D. W. Kung, B. A. Lanman, S. Kwon, *Tetrahedron Lett.* **2000**, *41*, 1359–1362.

[26] Observation of the emulsions with optical microscopy prior to the reaction (i.e., immediately before addition of the enzyme) revealed the following features: at 51 mM aldehyde (30 mM DHAP) the emulsions formulated with tetradecane and hexadecane were highly concentrated water-in-oil-type emulsions while the one formulated with squalane was a diluted oil-in-water emulsion; at 340 mM aldehyde (120 mM DHAP) all emulsions were diluted oil-in-water emulsions. During the progress of the enzymatic reaction, the highly concentrated water-in-oil emulsions became more fluid, changing progressively to diluted oil-in-water emulsions near the end of the reaction. From these preliminary observations it appears that the type of emulsion did not influence the reaction performance.

[27] M. D. Bednarski, E. S. Simon, N. Bischofberger, W. D. Fessner, M. J. Kim, W. Lees, T. Saito, H. Waldmann, G. M. Whitesides, *J. Am. Chem. Soc.* **1989**, *111*, 627–635.

[28] W.-D. Fessner, C. Walter, *Top. Curr. Chem.* **1996**, *184*, 97–194.

[29] The stability of DHAP in emulsions was measured without (i.e., blank experiment) and in the presence of either RAMA (35 U mL^{-1}) or aminoaldehyde **5** (50 mM) at pH 6.9. In the blank experiment, a 15% degradation of DHAP was observed after 24 h. In the presence of either RAMA or aldehyde, 30% degradation was detected after 24 h.

[30] W. J. Lees, G. M. Whitesides, *J. Org. Chem.* **1993**, *58*, 1887–1894.

[31] W. D. Fessner, G. Sinerius, A. Schneider, M. Dreyer, G. E. Schulz, J. Badia, J. Aguilar, *Angew. Chem.* **1991**, *103*, 596–599; *Angew. Chem. Int. Ed.* **1991**, *30*, 555–558.

[32] W. D. Fessner, J. Badia, O. Eyrisch, A. Schneider, G. Sinerius, *Tetrahedron Lett.* **1992**, *33*, 5231–5234.

[33] K. H. Choi, J. Shi, C. E. Hopkins, D. R. Tolan, K. N. Allen, *Biochemistry* **2001**, *40*, 13868–13875.

[34] W.-D. Fessner, A. Schneider, H. Held, G. Sinerius, C. Walter, M. Hixon, J. V. Schloss, *Angew. Chem.* **1996**, 108, 2366–2369; *Angew. Chem. Int. Ed.* **1996**, *35*, 2219–2221.

[35] J. A. Littlechild, H. C. Watson, *Trends Biochem. Sci.* **1993**, *18*, 36–39.

[36] A. C. Joerger, C. Gosse, W.-D. Fessner, G. E. Schulz, *Biochemistry* **2000**, *39*, 6033–6041.

[37] N. Matsumori, D. Kaneno, M. Murata, H. Nakamura, K. Tachibana, *J. Org. Chem.* **1999**, *64*, 866–876.

[38] K. K. C. Liu, T. Kajimoto, L. Chen, Z. Zhong, Y. Ichikawa, C. H. Wong, *J. Org. Chem.* **1991**, *56*, 6280–6289.

[39] T. Gefflaut, C. Blonski, J. Perie, M. Willson, *Prog. Biophys. Mol. Biol.* **1995**, *63*, 301–340.

[40] A. Dalby, Z. Dauter, J. A. Littlechild, *Protein Sci.* **1999**, *8*, 291–297.

[41] D. R. Hall, G. A. Leonard, C. D. Reed, C. I. Watt, A. Berry, W. N. Hunter, *J. Mol. Biol.* **1999**, *287*, 383–394.

[42] A possible diastereoisomer of **9** or **13** (15%) was detected but its relative configuration could not be identified unequivocally due to overlapping signals in the NMR spectra.

[43] F. G. Riddell in *Cyclic Organonitrogen Stereodynamics* (Eds.: J. B. Lambert, Y. Takeuchi), VCH, Weinheim, **1992**, pp. 159–165.

[44] At low temperatures (285 K), distinctive signals were observed in the high-field proton NMR spectrum for the corresponding linear **10** and the two five-membered ring conformers. Unfortunately, it was not possible to freeze the equilibrium between the two cyclic conformers and therefore the stereochemistry at C-2 could not be determined unequivocally. Moreover, the NMR spectra revealed the existence of only one of the two possible cyclic diastereoisomers, indicating that attack of the secondary amine on the ketone carbonyl exhibited face selectivity.

[45] Hydrogenation at atmospheric pressure for 2 h afforded the corresponding cyclic imine sugars.

[46] T. Kajimoto, L. Chen, K. K. C. Liu, C. H. Wong, *J. Am. Chem. Soc.* **1991**, *113*, 6678–6680.

[47] N. Asano, K. Yasuda, H. Kizu, A. Kato, J.-Q. Fan, R. J. Nash, G. W. J. Fleet, R. J. Molyneux, *Eur. J. Biochem.* **2001**, *268*, 35–41.

[48] S.-H. Jung, J.-H. Jeong, P. Miller, C.-H. Wong, *J. Org. Chem.* **1994**, *59*, 7182–7184.

[49] M. Kroemer, G. E. Schulz, *Acta Crystallogr. D Biol. Crystallogr.* **2002**, *58*, 824–832.

[50] H. M. Berman, J. Westbrook, Z. Feng, G. Gilliland, T. N. Bhat, H. Weissig, I. N. Shindyalov, P. E. Bourne, *Nucleic Acids Res.* **2000**, *28*, 235–242.

[51] H. Harada, O. Asano, T. Kawata, T. Inoue, T. Horizoe, N. Yasuda, K. Nagata, M. Murakami, J. Nagaoka, S. Kobayashi, *Bioorg. Med. Chem.* **2001**, *9*, 2709–2726.

[52] A. J. Geall, I. S. Blagbrough, *Tetrahedron* **2000**, *56*, 2449–2460.

[53] S. Fernandez, R. Brieva, F. Rebolledo, V. Gotor, *J. Chem. Soc. Perkin Trans. 1,* **1992**, 2885–2889.

[54] A. W. Konradi, S. J. Kemp, S. F. Pedersen, *J. Am. Chem. Soc.* **1994**, *116*, 1316–1323.

[55] N. Bischofberger, H. Waldmann, T. Saito, E. S. Simon, W. Lees, M. D. Bednarski, G. M. Whitesides, *J. Org. Chem.* **1988**, *53*, 3457–3465.

[56] M. Frigerio, M. Santagostino, S. Sputore, G. Palmisano, *J. Org. Chem.* **1995**, *60*, 7272–7276.

[57] F. Effenberger, A. Straub, *Tetrahedron Lett.* **1987**, *28*, 1641–1644.

[58] G. W. J. Fleet, P. W. Smith, *Tetrahedron* **1986**, *42*, 5685–5692.

[59] G. W. J. Fleet, L. E. Fellows, P. W. Smith, *Tetrahedron* **1987**, *43*, 979–990.

[60] G. W. J. Fleet, D. R. Witty, *Tetrahedron: Asymmetry* **1990**, *1*, 119–136.

[61] A. M. Scofield, L. E. Fellows, R. J. Nash, G. W. J. Fleet, *Life Sci.* **1986**, *39*, 645–650.

[62] Y. Banba, C. Abe, H. Nemoto, A. Kato, I. Adachi, H. Takahata, *Tetrahedron: Asymmetry* **2001**, *12*, 817–819.

[63] N. Asano, E. Tomioka, H. Kizu, K. Matsui, *Carbohydr. Res.* **1994**, *253*, 235–245.

[64] N. Asano, H. Kizu, K. Oseki, E. Tomioka, K. Matsui, M. Okamoto, M. Baba, *J. Med. Chem.* **1995**, *38*, 2349–2356.

[65] N. Asano, T. Yamashita, K. Yasuda, K. Ikeda, H. Kizu, Y. Kameda, A. Kato, R. J. Nash, H. S. Lee, K. S. Ryu, *J. Agric. Food Chem.* **2001**, *49*, 4208–4213.

[66] A. N. Hulme, C. H. Montgomery, D. K. Henderson, *J. Chem. Soc. Perkin Trans. 1* **2000**, 1837–1841.

[67] Y. F. Wang, D. P. Dumas, C. H. Wong, *Tetrahedron Lett.* **1993**, *34*, 403–406.

[68] A. M. Palmer, V. Jager, *Eur. J. Org. Chem.* **2001**, 2547–2558.

[69] R. J. Molyneux, Y. T. Pan, J. E. Tropea, A. D. Elbein, C. H. Lawyer, D. J. Hughes, G. W. J. Fleet, *J. Nat. Prod.* **1993**, *56*, 1356–1364.

[70] K. Yasuda, H. Kizu, T. Yamashita, Y. Kameda, A. Kato, R. J. Nash, G. W. J. Fleet, R. J. Molyneux, N. Asano, *J. Nat. Prod.* **2002**, *65*, 198–202.

[71] P. Bisseret, C. Bouix-Peter, O. Jacques, S. Henriot, J. Eustache, *Org. Lett.* **1999**, *1*, 1181–1182.

[72] P. A. M. Van der Klein, W. Filemon, H. J. G. Broxterman, G. A. Van der Marel, J. H. Van Boom, *Synth. Commun.* **1992**, *22*, 1763–1771.

[73] J. J. Naleway, C. R. H. Raetz, L. Anderson, *Carbohydr. Res.* **1988**, *179*, 199–209.

[74] Y. Huang, D. R. Dalton, P. J. Carroll, *J. Org. Chem.* **1997**, *62*, 372–376.

[75] M. Lombardo, S. Fabbroni, C. Trombini, *J. Org. Chem.* **2001**, *66*, 1264–1268.

[76] G. W. J. Fleet, A. Karpas, R. A. Dwek, L. E. Fellows, A. S. Tyms, S. Petursson, S. K. Namgoong, N. G. Ramsden, P. W. Smith, J. C. Son, *FEBS Lett.* **1988**, *237*, 128–132.

[77] G. W. J. Fleet, S. J. Nicholas, P. W. Smith, S. V. Evans, L. E. Fellows, R. J. Nash, *Tetrahedron Lett.* **1985**, *26*, 3127–3130.

[78] D. Wyn, C. Jones, R. J. Nash, E. A. Bell, J. M. Williams, *Tetrahedron Lett.* **1985**, *26*, 3125–3126.

[79] N. Ikota, A. Hanaki, *Chem. Pharm. Bull.* **1987**, *35*, 2140–2143.

[80] S. Takano, M. Moriya, K. Ogasawara, *Tetrahedron: Asymmetry* **1992**, *3*, 681–684.

[81] T. Sifferlen, A. Defoin, J. Streith, D. Le Nouen, C. Tarnus, I. Dosbaa, M.-J. Foglietti, *Tetrahedron* **2000**, *56*, 971–978.

[82] A. Defoin, T. Sifferlen, J. Streith, I. Dosbaa, M.-J. Foglietti, *Tetrahedron: Asymmetry* **1997**, *8*, 363–366.

Received: March 19, 2003 [F4966]

